LHAASO：与强相作用相关研究

张寿山

中国科学院高能物理研究所

Opportunities and Ideas at the QCD Frontier
2025/04/07-11，中国高等科学技术中心

如何探测宇宙线线?

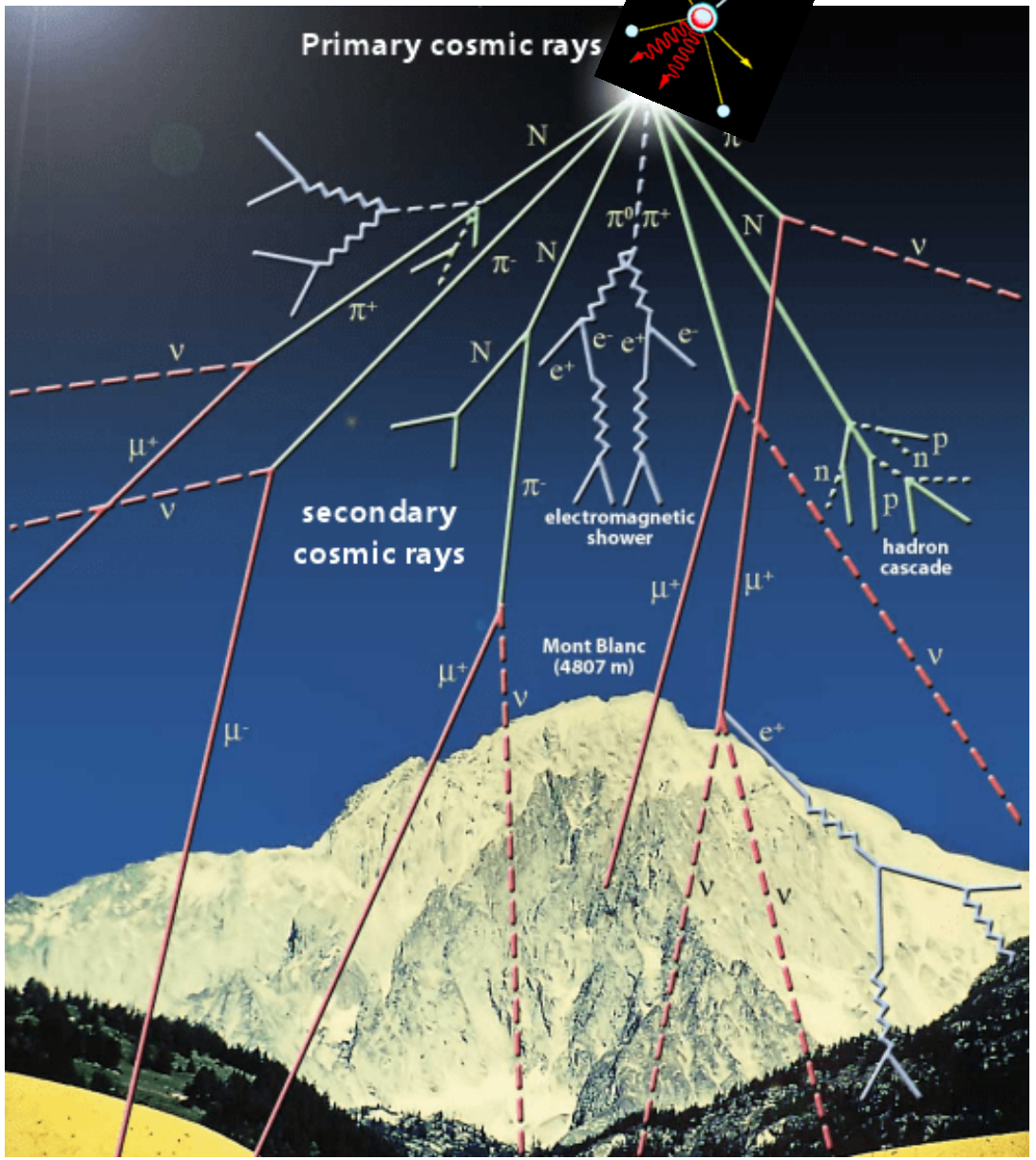

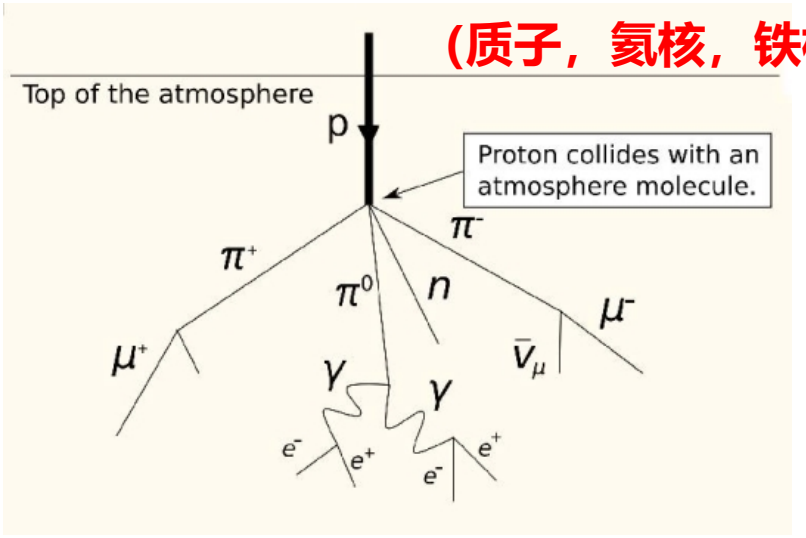

（质子，氦核，铁核等核子）

Development of gamma–ray air showers

伽马光子

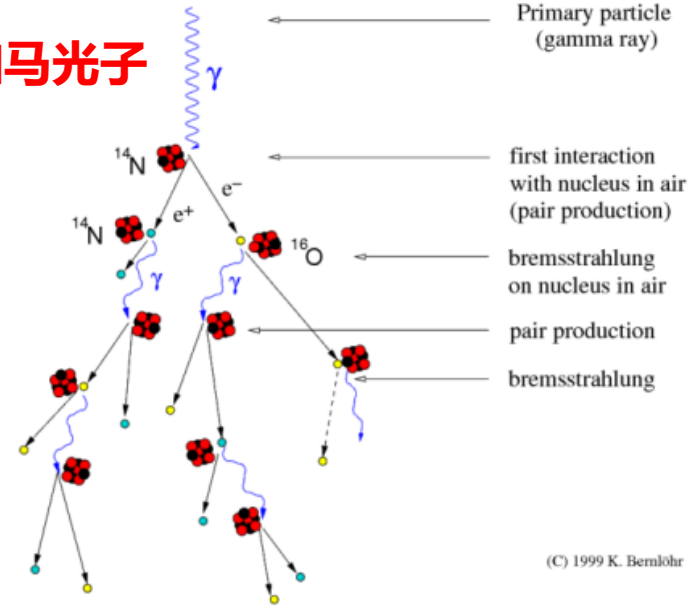

次级粒子：

正负电子、

伽马光子、

强子、

μ子、

中微子、

荧光、

Cherenkov光。

Interaction studies at LHC

Cosmic-ray (target-rest frame)

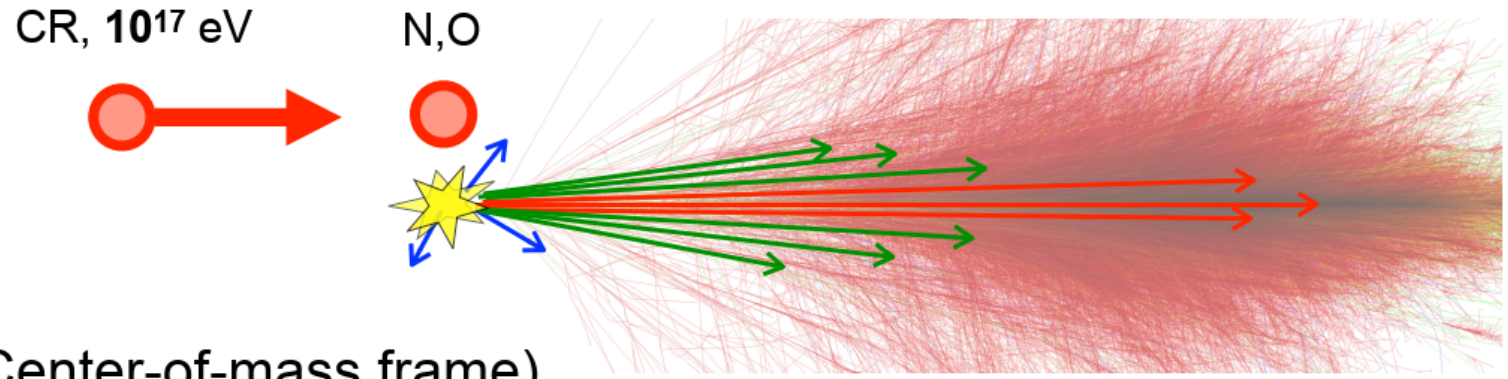

LHC(Center-of-mass frame)

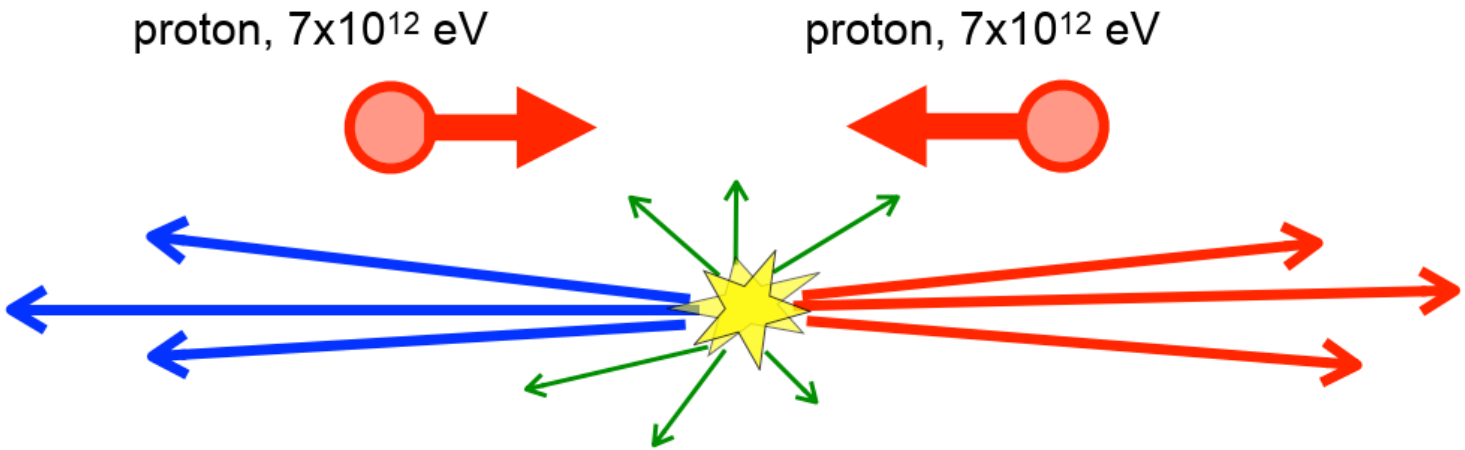

质子-反质子对撞机
单一储存环

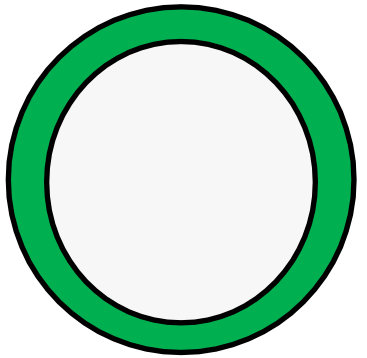

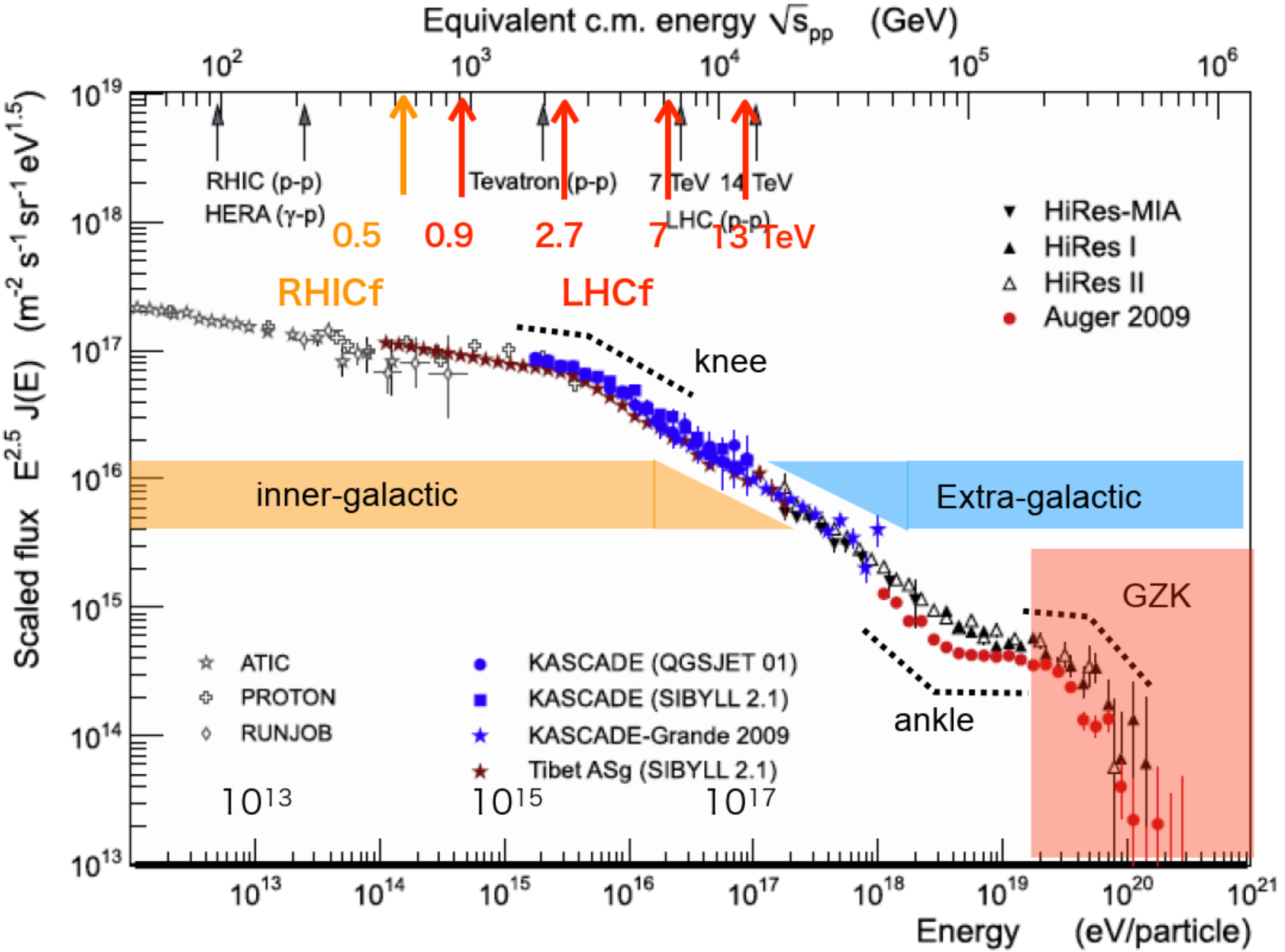
Equivalent c.m. energy $\sqrt{s_{pp}}$ (GeV)
10^2
10^3
10^4
10^5
10^6
RHIC (p-p)
HERA (γ-p)
Tevatron (p-p)
7 TeV
14 TeV
LHC (p-p)
0.5
0.9
2.7
7
13 TeV
RHICf
LHCf
HiRes-MIA
HiRes I
HiRes II
Auger 2009
knee
inner-galactic
Extra-galactic
GZK
ankle
ATIC
PROTON
RUNJOB
KASCADE (QGSJET 01)
KASCADE (SIBYLL 2.1)
KASCADE-Grande 2009
Tibet ASg (SIBYLL 2.1)
10^{13}
10^{15}
10^{17}
Scaled flux $E^{2.5}$ J(E) $(m^{-2}\ s^{-1}\ sr^{-1}\ eV^{1.5})$
10^{19}
10^{18}
10^{17}
10^{16}
10^{15}
10^{14}
10^{13}
10^{13}
10^{14}
10^{15}
10^{16}
10^{17}
10^{18}
10^{19}
10^{20}
10^{21}
Energy (eV/particle)

The Site

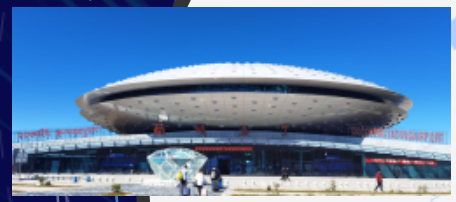

Bird's eye view of LHAASO, 2021-08

- **Location: 29o21' 27.6" N , 100o08'19.6" E**
- **Altitude: 4410 m**
- **2021-07 completed built and in operation**

LHAASO, *Nature Astronomy* **5:849 (2021)**

(Aug. 2018, at 4410 m a.s.l.)

LHAASO: Multi-Messenger Collaboration Network

The LHAASO collaboration has signed MOUs with 8 international detector collaboration.

ANTARES (NT)

KM3Net (NT)

LST/CTA-N (CT)

MAGIC(CT)

Baikal-GVD (NT)

VERITAS (CT)

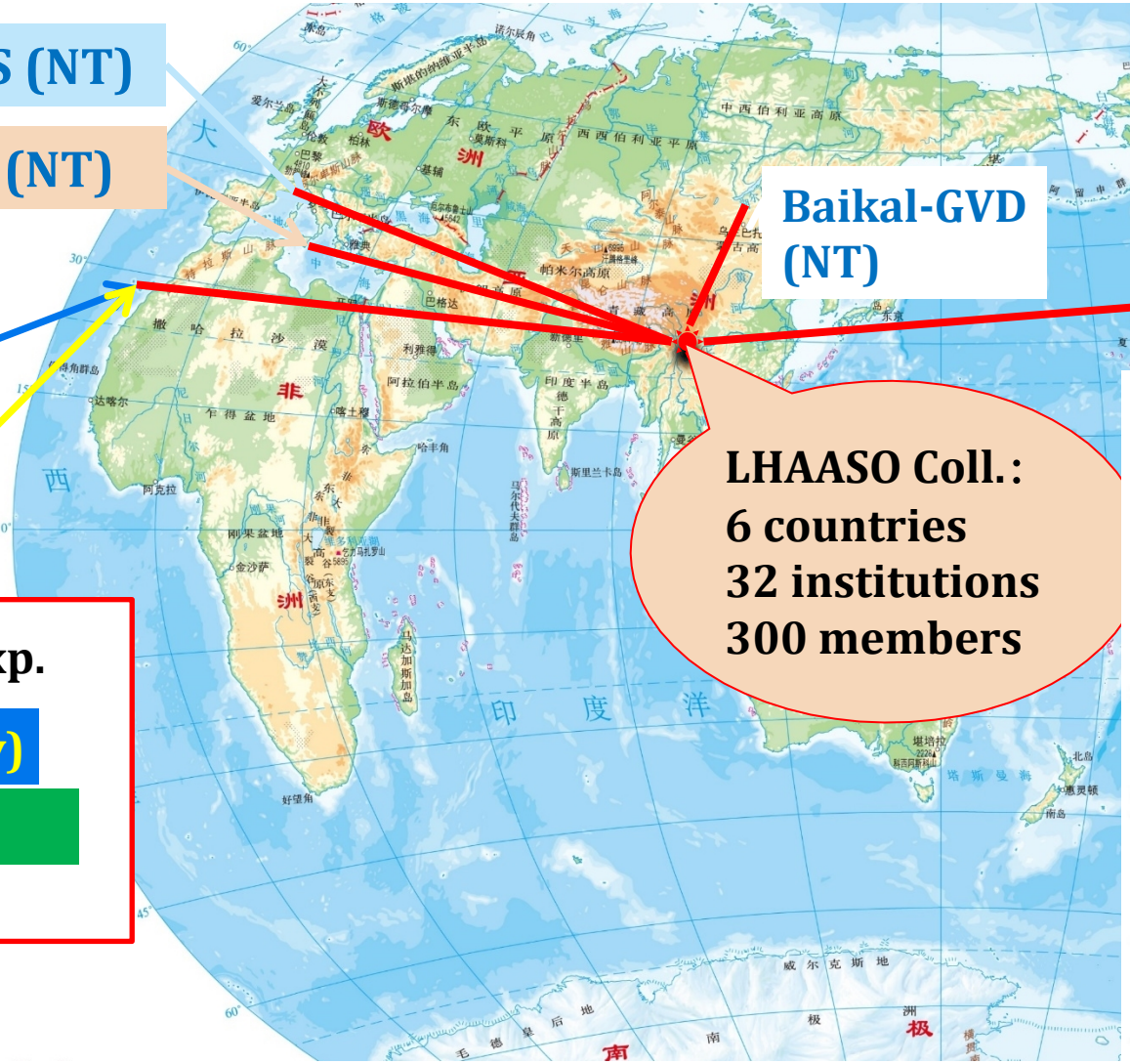

LHAASO Coll.:
6 countries
32 institutions
300 members

Space borne Exp.

eROSITA(X-ray)

DAMPE(γ-ray, CR)

Zhen Cao,[1,2,3] F. Aharonian,[4,5] Q. An,[6,7] Axikegu,[8] L.X. Bai,[9] Y.X. Bai,[1,3] Y.W. Bao,[10] D. Bastieri,[11] X.J. Bi*,[1,2,3] Y.J. Bi,[1,3] H. Cai,[12] J.T. Cai,[11] Zhe Cao,[6,7] J. Chang,[13] J.F. Chang,[1,3,6] B.M. Chen,[14] E.S. Chen*,[1,2,3] J. Chen,[9] Liang Chen,[1,2,3] Liang Chen,[15] Long Chen,[8] M.J. Chen,[1,3] M.L. Chen,[1,3,6] Q.H. Chen,[8] S.H. Chen,[1,2,3] S.Z. Chen,[1,3] T.L. Chen,[16] X.L. Chen,[1,2,3] Y. Chen,[10] N. Cheng,[1,3] Y.D. Cheng,[1,3] S.W. Cui,[14] X.H. Cui,[17] Y.D. Cui,[18] B. D'Ettorre Piazzoli,[19] B.Z. Dai,[20] H.L. Dai,[1,3,6] Z.G. Dai,[7] Danzengluobu,[16] D. della Volpe,[21] X.J. Dong,[1,3] K.K. Duan,[13] J.H. Fan,[11] Y.Z. Fan,[13] Z.X. Fan,[1,3] J. Fang,[20] K. Fang,[1,3] C.F. Feng,[22] L. Feng,[13] S.H. Feng,[1,3] Y.L. Feng,[13] B. Gao,[1,3] C.D. Gao,[22] L.Q. Gao*,[1,2,3] Q. Gao,[16] W. Gao,[22] M.M. Ge,[20] L.S. Geng,[1,3] G.H. Gong,[23] Q.B. Gou,[1,3] M.H. Gu,[1,3,6] F.L. Guo,[15] J.G. Guo,[1,2,3] X.L. Guo,[8] Y.Q. Guo,[1,3] Y.Y. Guo,[1,2,3,13] Y.A. Han,[24] H.H. He,[1,2,3] H.N. He,[13] J.C. He,[1,2,3] S.L. He,[11] X.B. He,[18] Y. He,[8] M. Heller,[21] Y.K. Hor,[18] C. Hou,[1,3] X. Hou,[25] H.B. Hu,[1,2,3] S. Hu,[9] S.C. Hu,[1,2,3] X.J. Hu,[23] D.H. Huang,[8] Q.L. Huang,[1,3] W.H. Huang,[22] X.T. Huang,[22] X.Y. Huang,[13] Z.C. Huang,[8] F. Ji,[1,3] X.L. Ji,[1,3,6] H.Y. Jia,[8] K. Jiang,[6,7] Z.J. Jiang,[20] C. Jin,[1,2,3] T. Ke,[1,3] D. Kuleshov,[26] K. Levochkin,[26] B.B. Li,[14] Cheng Li,[6,7] Cong Li,[1,3] F. Li,[1,3,6] H.B. Li,[1,3] H.C. Li,[1,3] H.Y. Li,[7,13] Jian Li,[7] Jie Li,[1,3,6] K. Li,[1,3] W.L. Li,[22] X.R. Li,[1,3] Xin Li,[6,7] Xin Li,[8] Y. Li,[9] Y.Z. Li,[1,2,3] Zhe Li,[1,3] Zhuo Li,[27] E.W. Liang,[28] Y.F. Liang,[28] S.J. Lin,[18] B. Liu,[7] C. Liu,[1,3] D. Liu,[22] H. Liu,[8] H.D. Liu,[24] J. Liu,[1,3] J.L. Liu,[29] J.S. Liu,[18] J.Y. Liu,[1,3] M.Y. Liu,[16] R.Y. Liu,[10] S.M. Liu,[8] W. Liu,[1,3] Y. Liu,[11] Y.N. Liu,[23] Z.X. Liu,[9] W.J. Long,[8] R. Lu,[20] H.K. Lv,[1,3] B.Q. Ma,[27] L.L. Ma,[1,3] X.H. Ma,[1,3] J.R. Mao,[25] A. Masood,[8] Z. Min,[1,3] W. Mitthumsiri,[30] T. Montaruli,[21] Y.C. Nan,[22] B.Y. Pang,[8] P. Pattarakijwanich,[30] Z.Y. Pei,[11] M.Y. Qi,[1,3] Y.Q. Qi,[14] B.Q. Qiao,[1,3] J.J. Qin,[7] D. Ruffolo,[30] V. Rulev,[26] A. Sáiz,[30] L. Shao,[14] O. Shchegolev,[26,31] X.D. Sheng,[1,3] J.R. Shi,[1,3] H.C. Song,[27] Yu.V. Stenkin,[26,31] V. Stepanov,[26] Y. Su,[13] Q.N. Sun,[8] X.N. Sun,[28] Z.B. Sun,[32] P.H.T. Tam,[18] Z.B. Tang,[6,7] W.W. Tian,[2,17] B.D. Wang,[1,3] C. Wang,[32] H. Wang,[8] H.G. Wang,[11] J.C. Wang,[25] J.S. Wang,[29] L.P. Wang,[22] L.Y. Wang,[1,3] R.N. Wang,[8] W. Wang,[18] W. Wang,[12] X.G. Wang,[28] X.J. Wang,[1,3] X.Y. Wang,[10] Y. Wang,[8] Y.D. Wang,[1,3] Y.J. Wang,[1,3] Y.P. Wang,[1,2,3] Z.H. Wang,[9] Z.X. Wang,[20] Zhen Wang,[29] Zheng Wang,[1,3,6] D.M. Wei,[13] J.J. Wei,[13] Y.J. Wei,[1,2,3] T. Wen,[20] C.Y. Wu,[1,3] H.R. Wu,[1,3] S. Wu,[1,3] W.X. Wu,[8] X.F. Wu,[13] S.Q. Xi,[1,3] J. Xia,[7,13] J.J. Xia,[8] G.M. Xiang,[2,15] D.X. Xiao,[16] G. Xiao,[1,3] H.B. Xiao,[11] G.G. Xin,[12] Y.L. Xin,[8] Y. Xing,[15] D.L. Xu,[29] R.X. Xu,[27] L. Xue,[22] D.H. Yan,[25] J.Z. Yan,[13] C.W. Yang,[9] F.F. Yang,[1,3,6] J.Y. Yang,[18] L.L. Yang,[18] M.J. Yang,[1,3] R.Z. Yang,[7] S.B. Yang,[20] Y.H. Yao,[9] Z.G. Yao,[1,3] Y.M. Ye,[23] L.Q. Yin,[1,3] N. Yin,[22] X.H. You,[1,3] Z.Y. You,[1,2,3] Y.H. Yu,[22] Q. Yuan*,[13] H.D. Zeng,[13] T.X. Zeng,[1,3,6] W. Zeng,[20] Z.K. Zeng,[1,2,3] M. Zha,[1,3] X.X. Zhai,[1,3] B.B. Zhang,[10] H.M. Zhang,[10] H.Y. Zhang,[22] J.L. Zhang,[17] J.W. Zhang,[9] L.X. Zhang,[11] Li Zhang,[20] Lu Zhang,[14] P.F. Zhang,[20] P.P. Zhang,[14] R. Zhang,[7,13] S.R. Zhang,[14] S.S. Zhang,[1,3] X. Zhang,[10] X.P. Zhang,[1,3] Y.F. Zhang,[8] Y.L. Zhang,[1,3] Yi Zhang*,[1,13] Yong Zhang,[1,3] B. Zhao,[8] J. Zhao,[1,3] L. Zhao,[6,7] L.Z. Zhao,[14] S.P. Zhao*,[13,22] F. Zheng,[32] Y. Zheng,[8] B. Zhou,[1,3] H. Zhou,[29] J.N. Zhou,[15] P. Zhou,[10] R. Zhou,[9] X.X. Zhou,[8] C.G. Zhu,[22] F.R. Zhu,[8] H. Zhu,[17] K.J. Zhu,[1,2,3,6] and X. Zuo[1,3]

High Energy Cosmic Rays

Large High Altitude Air Shower Observatory (LHAASO)

LHAASO Physics Topics

- Gamma Ray Astronomy
- Charged CRs measurement
- New Physics Frontier

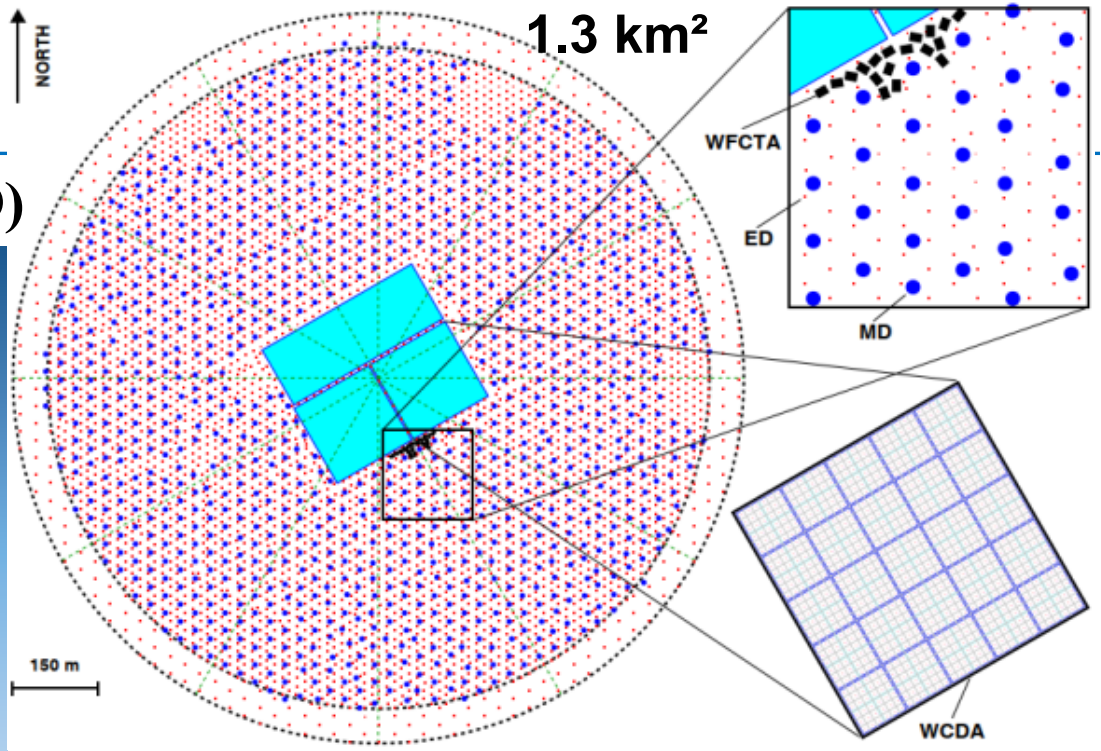

Hybrid Detection of EAS

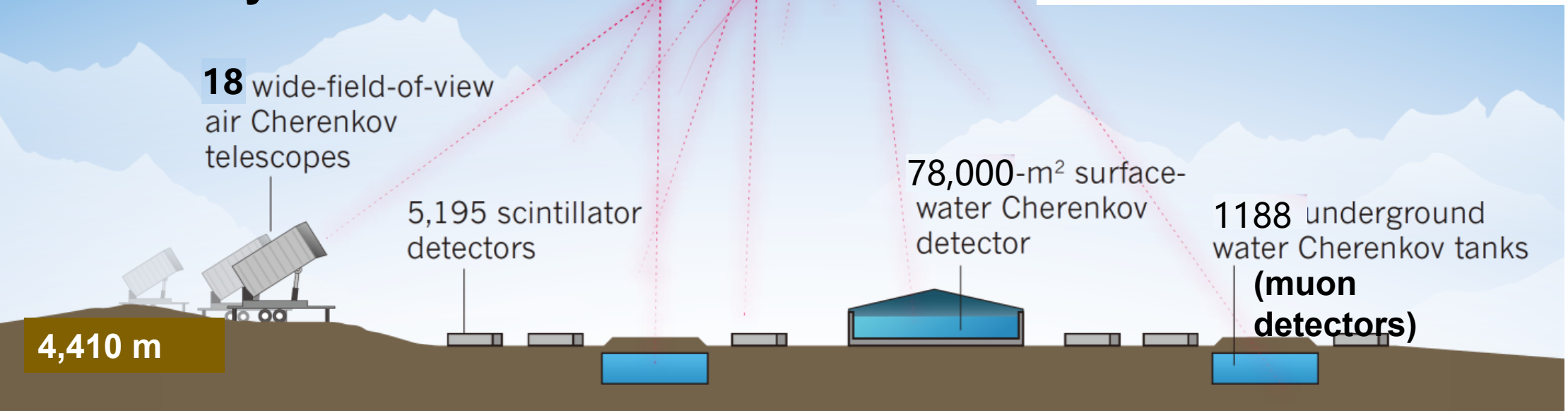

高海拔宇宙线观测站（LHAASO）

- 地点：四川甘孜州稻城海子山
- 海拔: 4410 m

  “膝区”宇宙线测量的理想位置，测量精度高
- **2021年7月全面建成，2023年5月通过国家验收**

地面粒子探测器阵列(KM2A)

最灵敏的超高能伽马望远镜

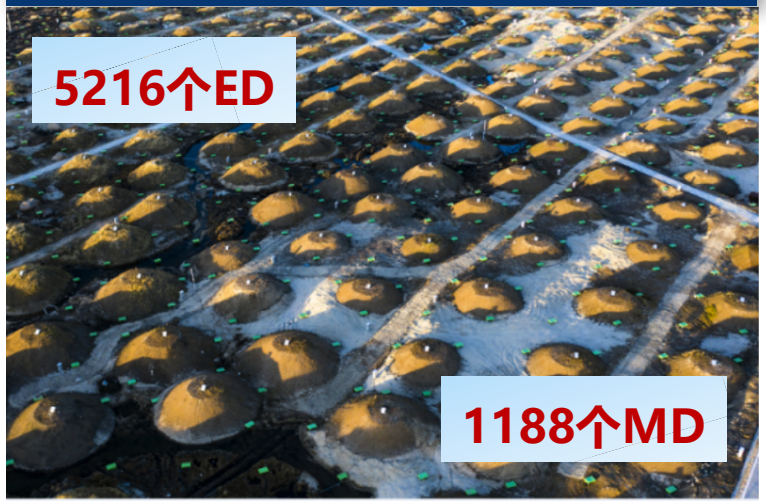

水切伦科夫探测器阵列(WCDA)

最灵敏的甚高能伽马巡天望远镜

广角切伦科夫望远镜阵列(WFCTA)

能量覆盖最宽的高能宇宙线立体装置

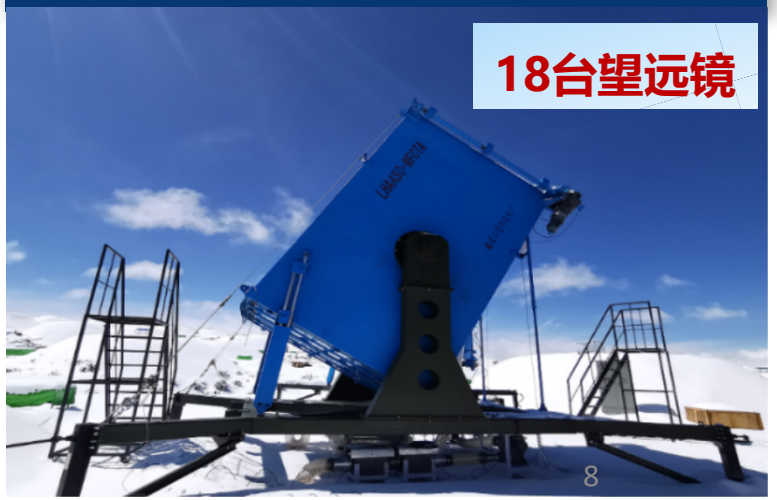

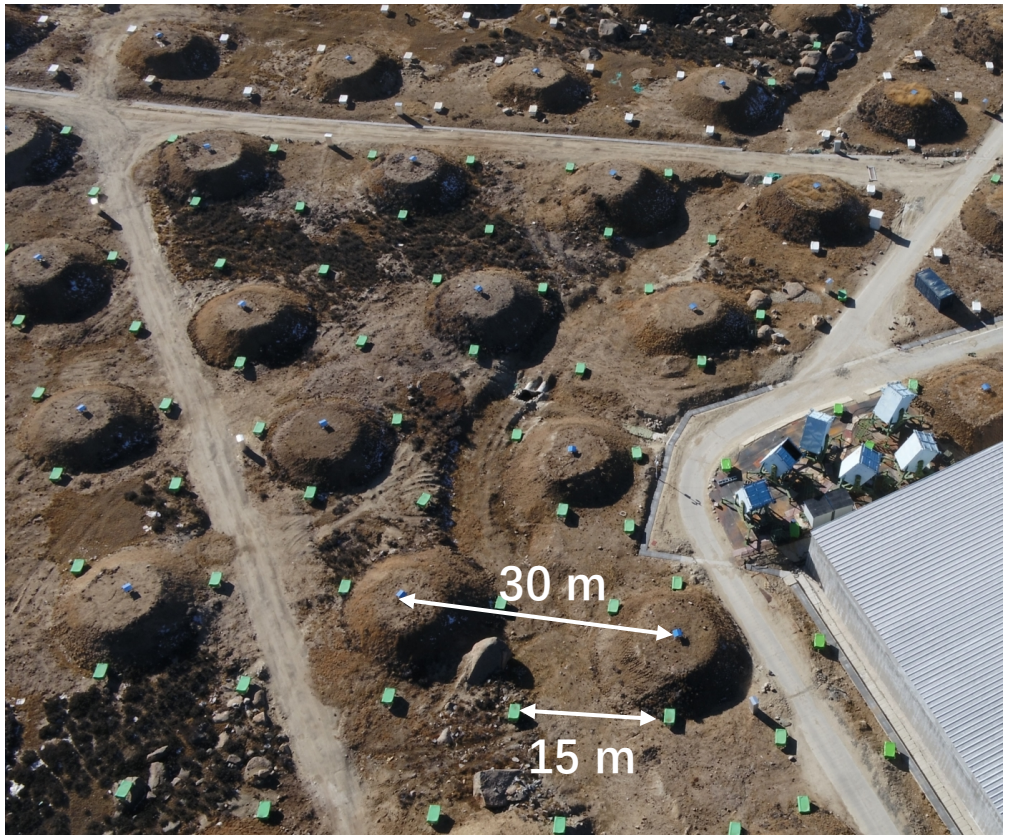

KM2A: 1.36 (km)^2

- 5195 EDs
  - 1 m^2 each
  - 15 m spacing
- 1188 MDs
  - 36 m^2 each
  - 30 m spacing

Scintillator Detectors （ED）

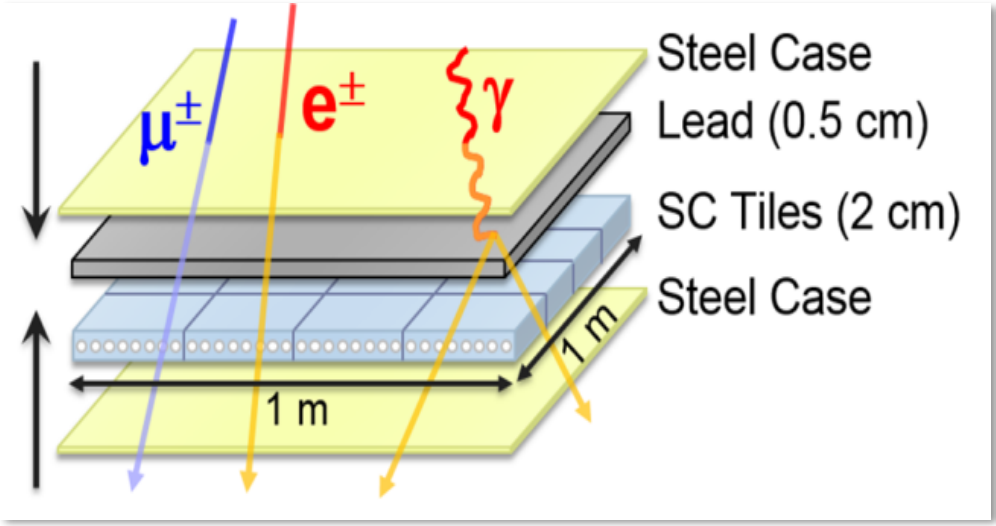

Muon detector（MD）

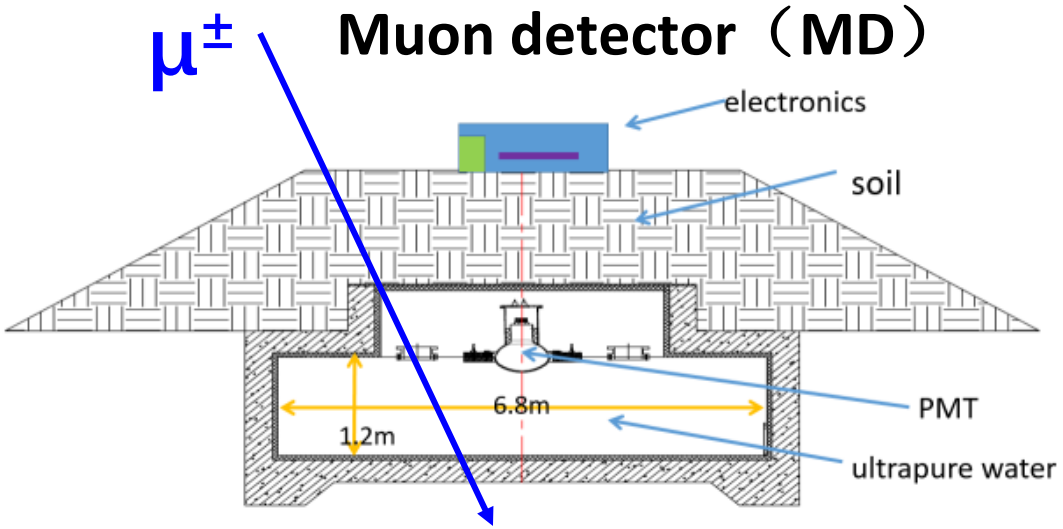

Inner View of one ED

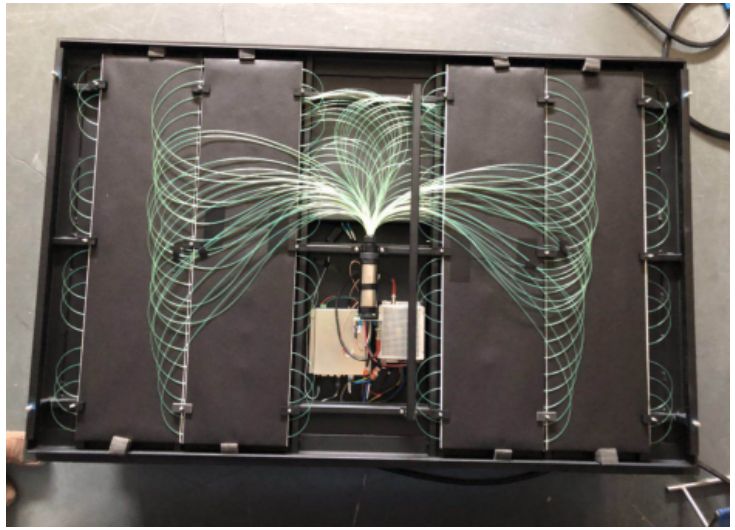

粒子鉴别参数：μ子

Active Area for Muons vs. Array Area: 4%

~1 PeV CR event: many muons

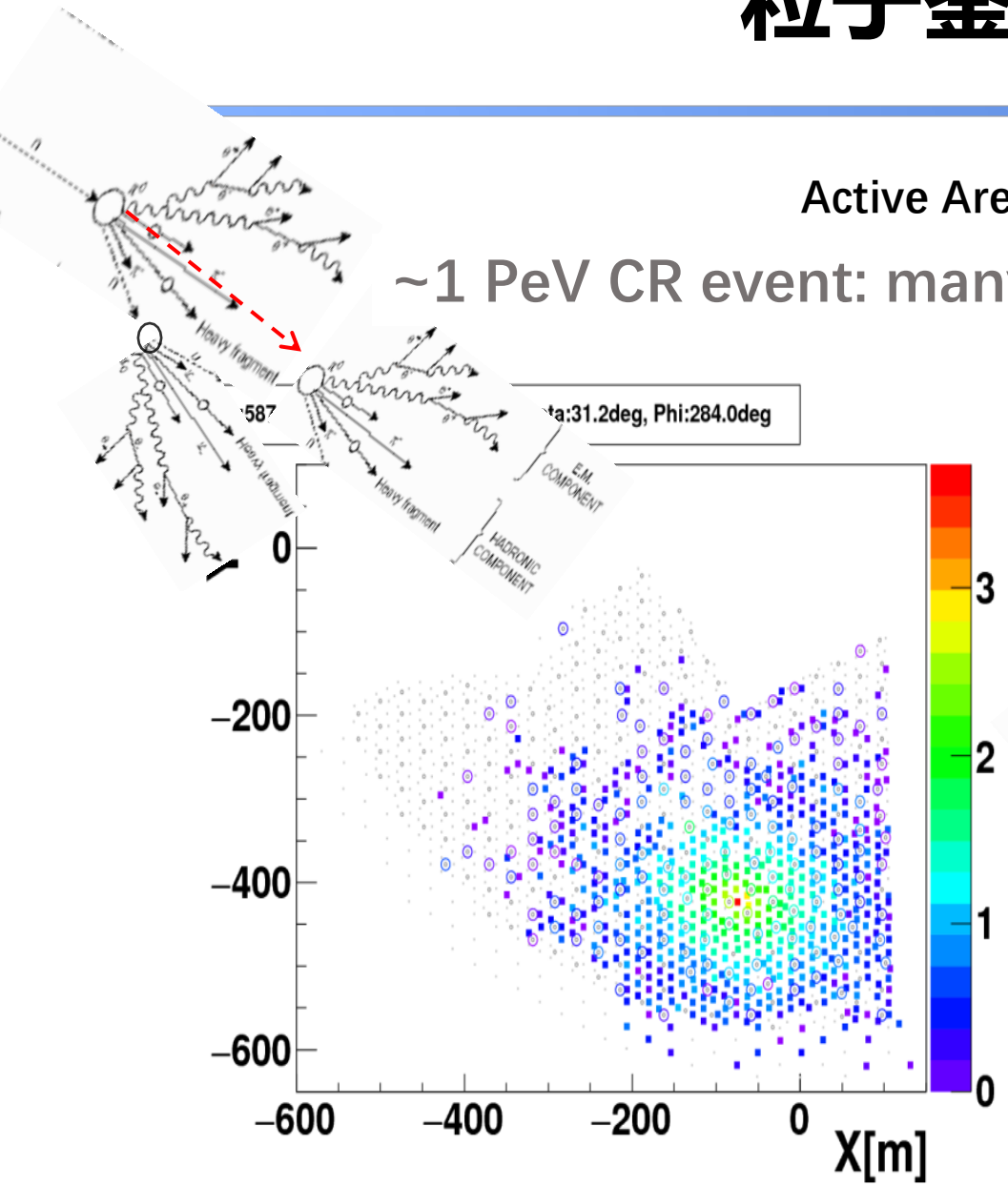

~ 1 PeV γ–ray event： very few muons from the Crab

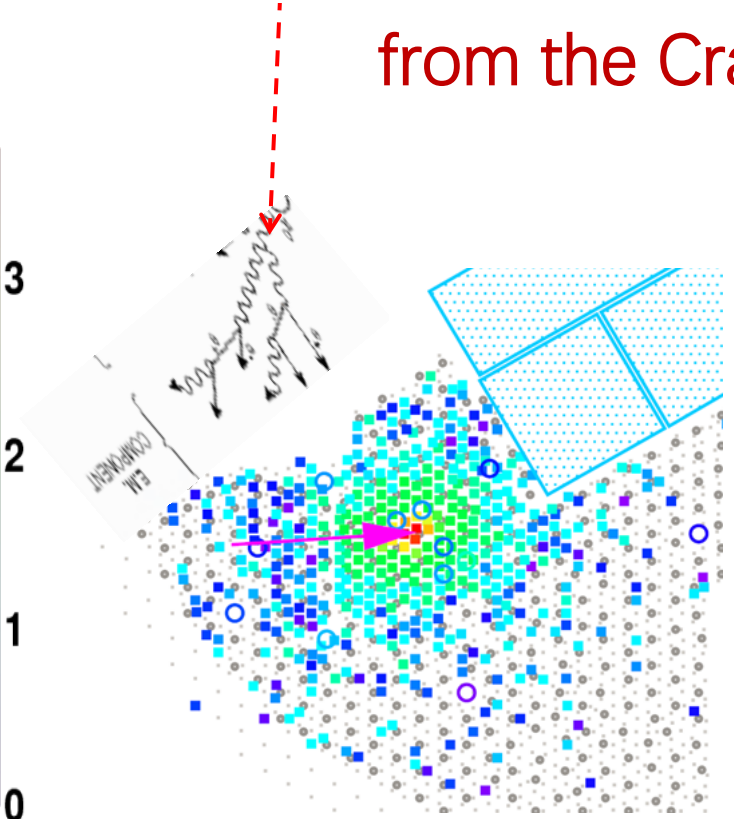

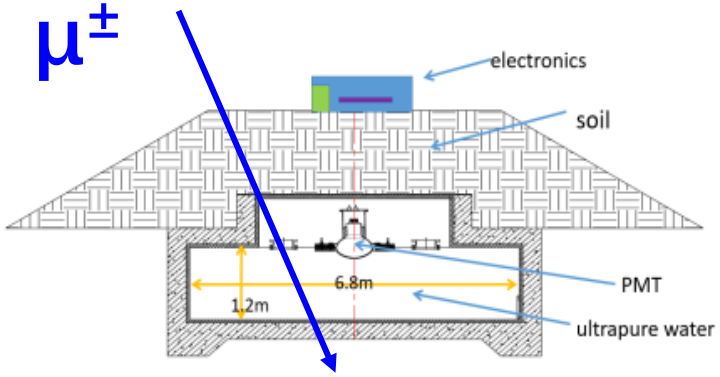

Muon detector（MD）

Muon information from LHAASO

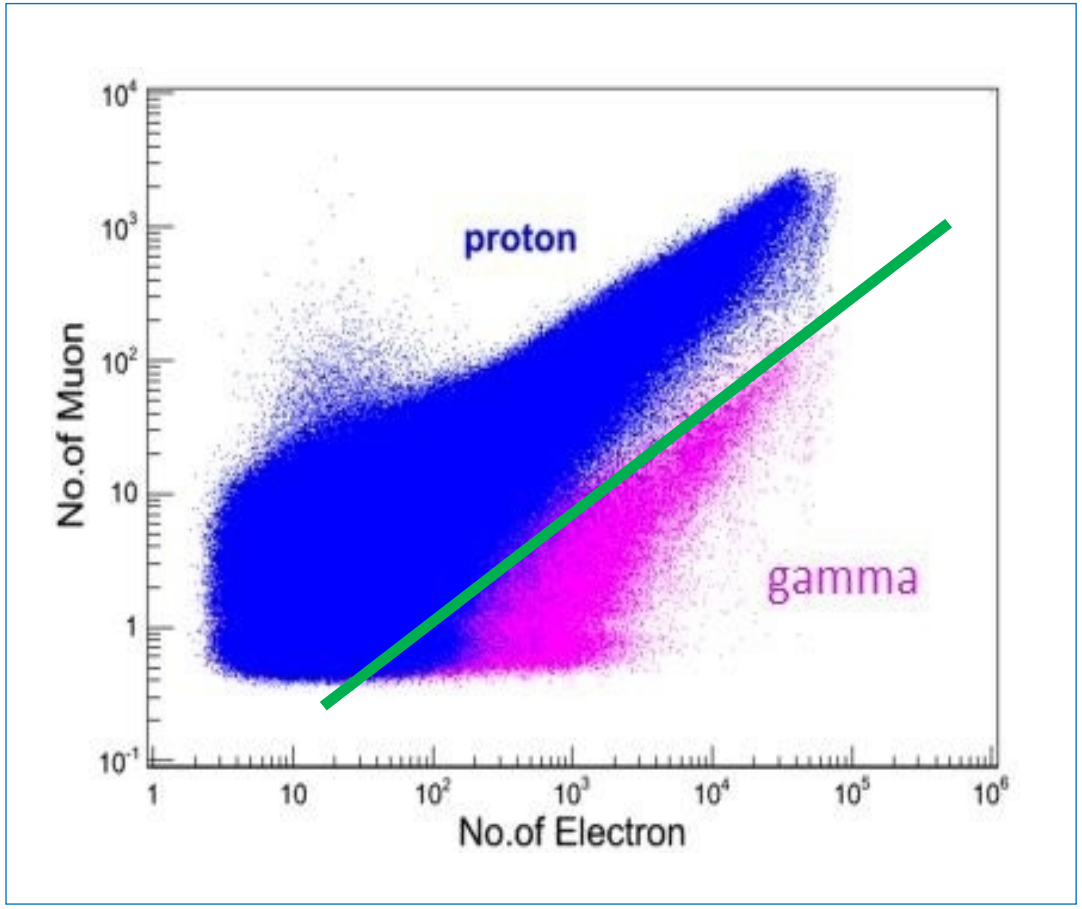

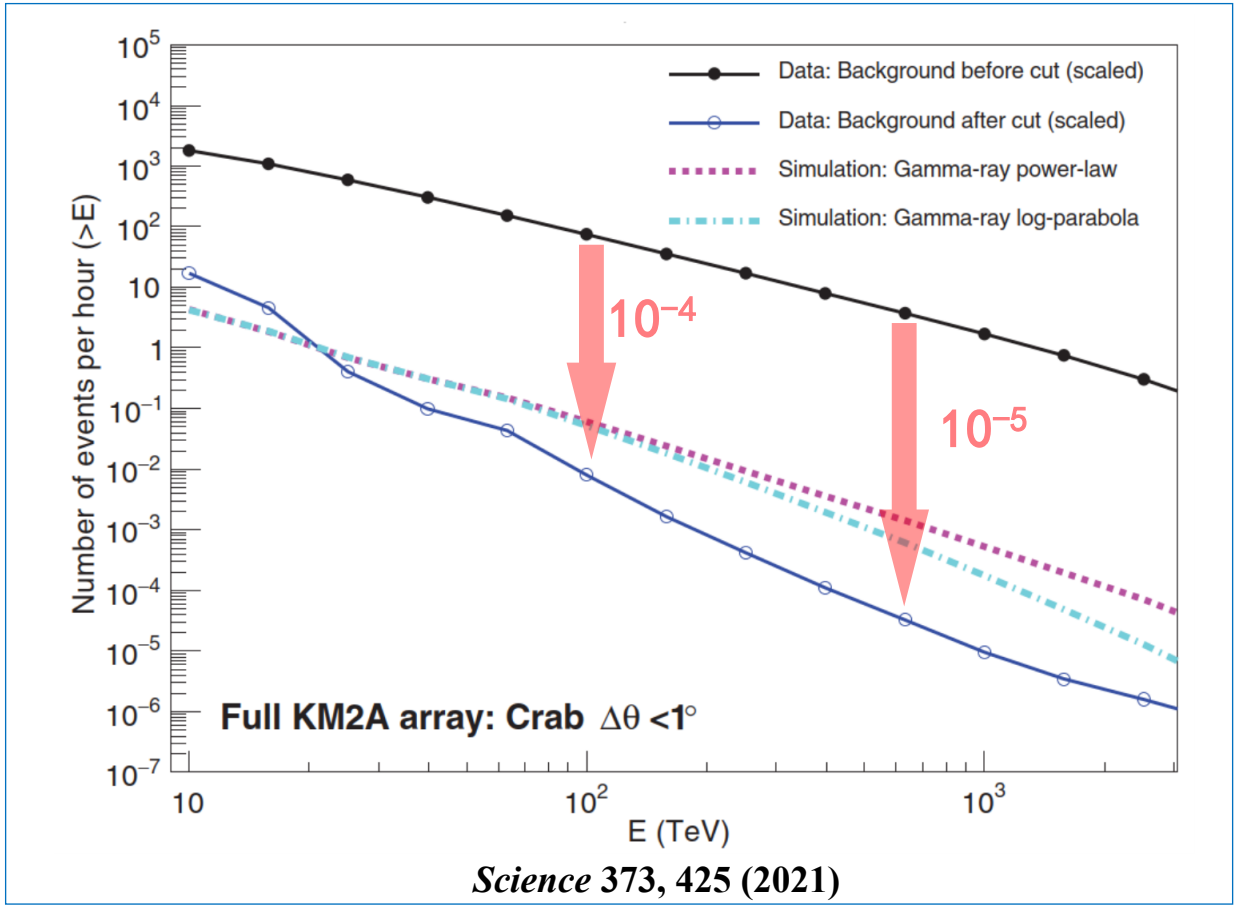

Science 373, 425 (2021)

Water Cherenkov Detector Array (WCDA)

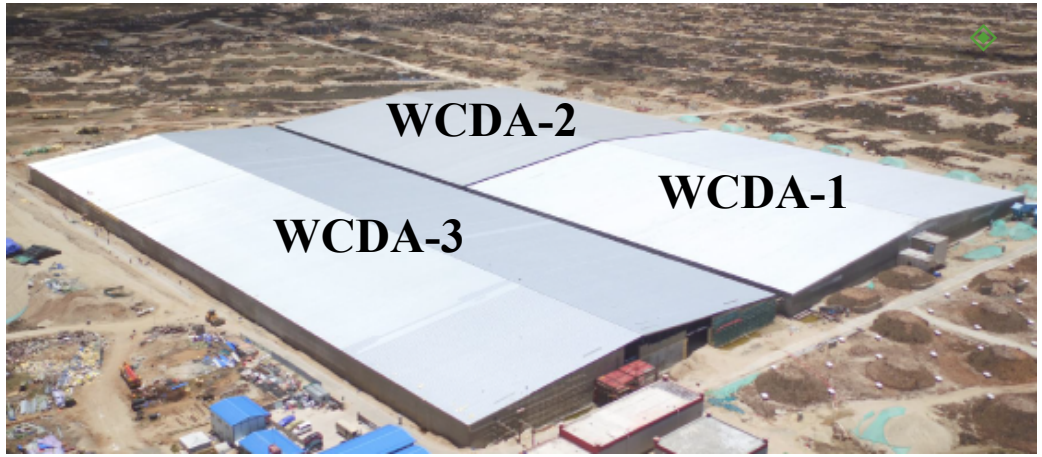

- Energy rang
- WCDA-1
  - 300 GeV – 10 PeV
- WCDA-2 and WCDA-3
  - 100 GeV - 10 TeV

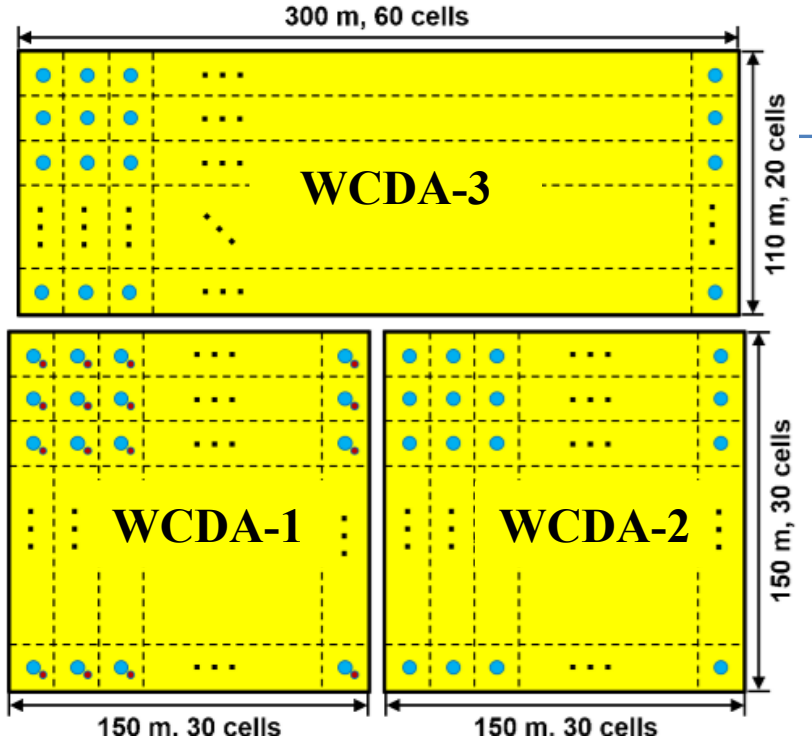

- Total area: $78,000m^2$
- Total units: 3,120
- Unit size: $5m \times 5m \times 4.4m$
- Two type of PMTs in each unit:
  - 8 inches and 1.5 inches for WCDA-1
  - 20 inches and 3 inches for WCDA-2 and WCDA-3

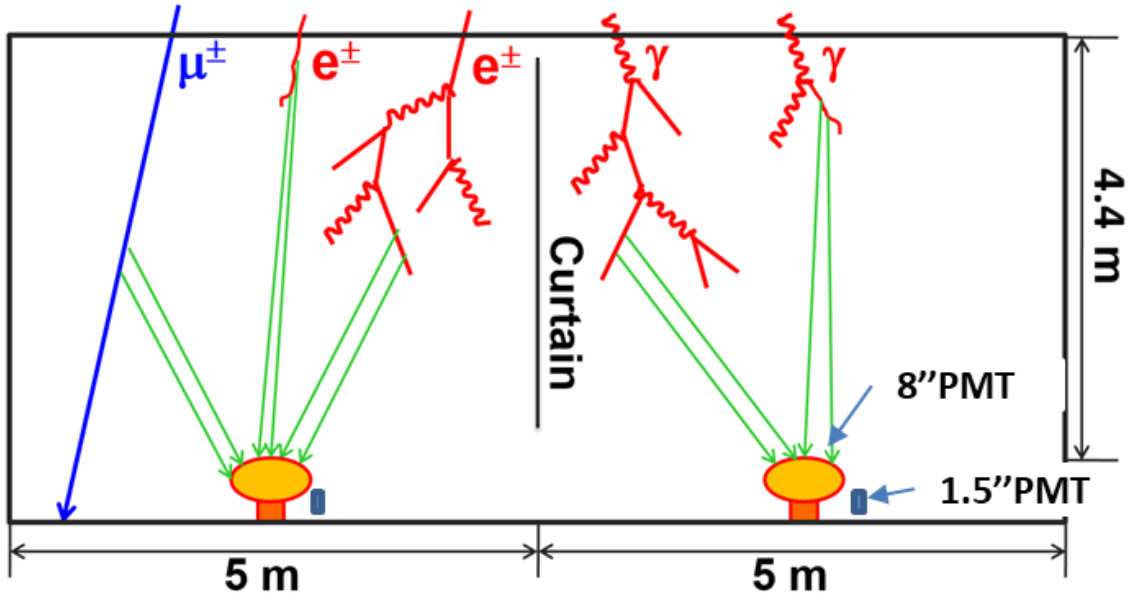

Inside of WCDA-3

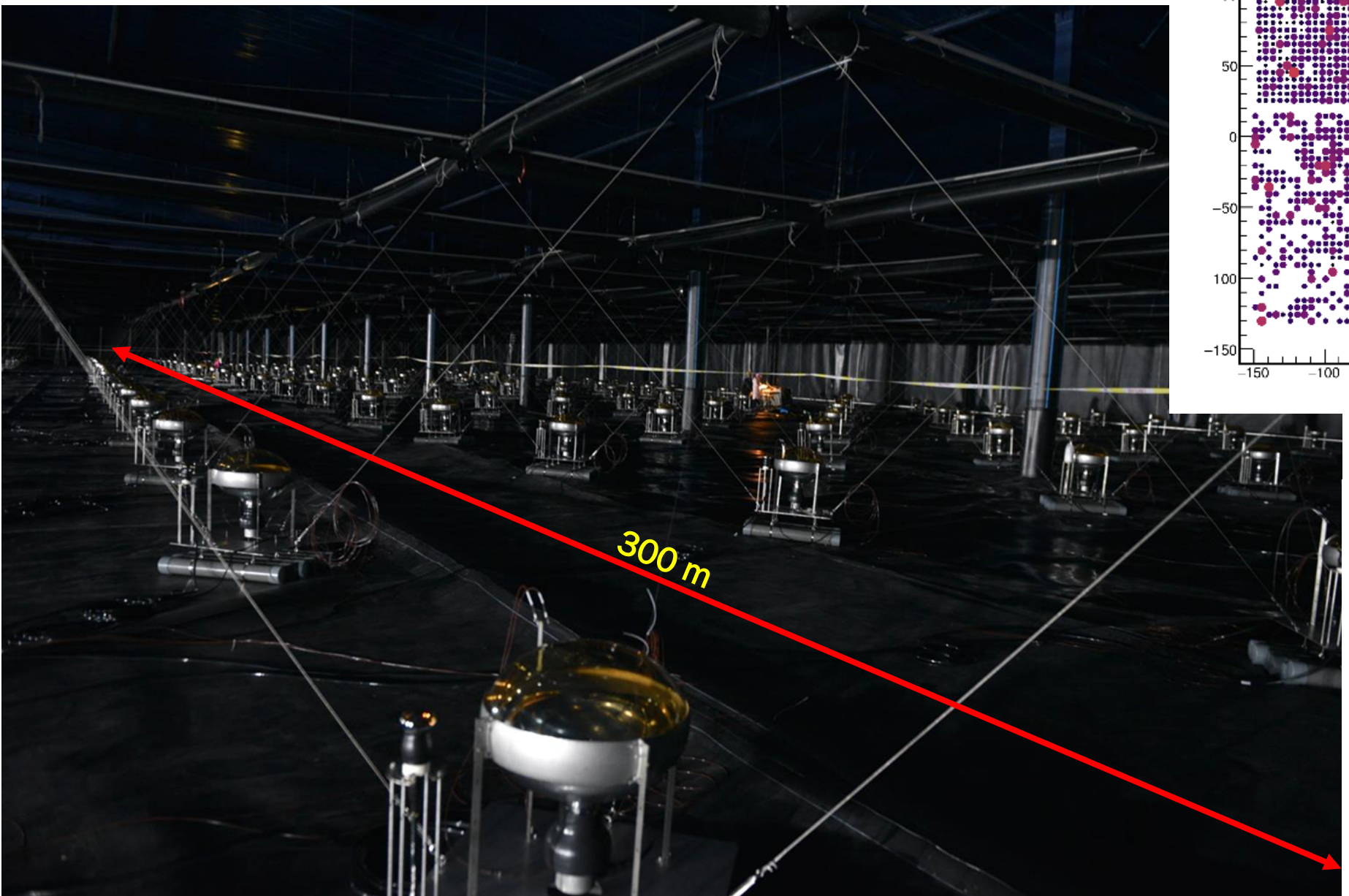

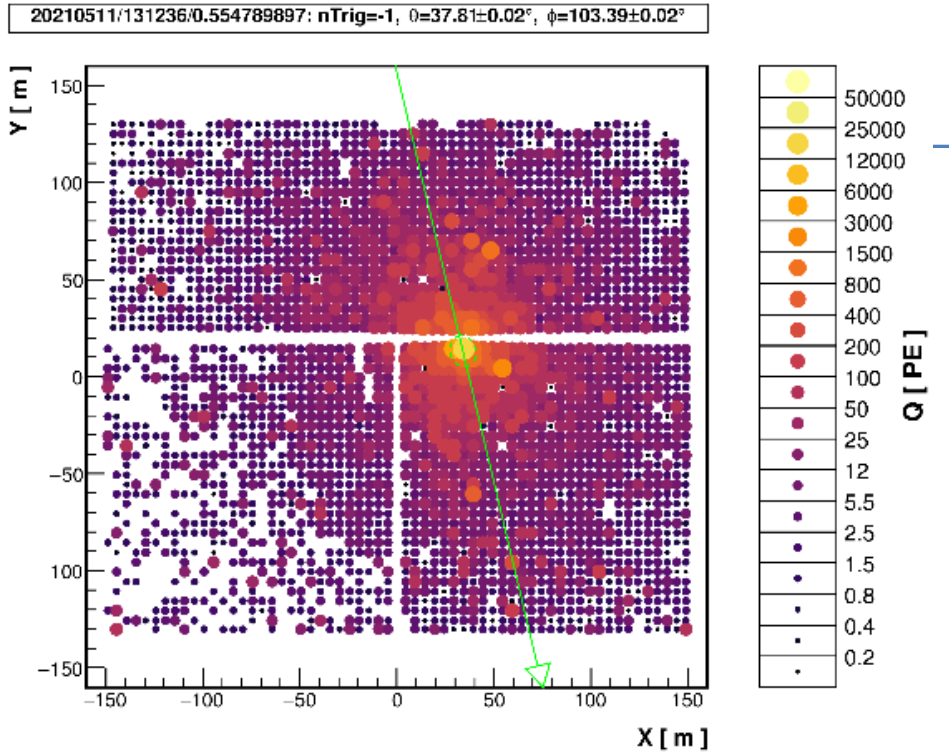

- WCDA-1 started operating in April 2019
- WCDA-2 started operating in January 2020
- WCDA-3 started operating in March 2021

Wide Field of View Cherenkov Telescope (WFCTA)

◆ Telescope parameters:

- ~5 m^2 spherical mirror
- Camera: 32×32 SiPMs array
- FOV: $16^\circ \times 16^\circ$
- Pixel size: 0.5°

Mirror

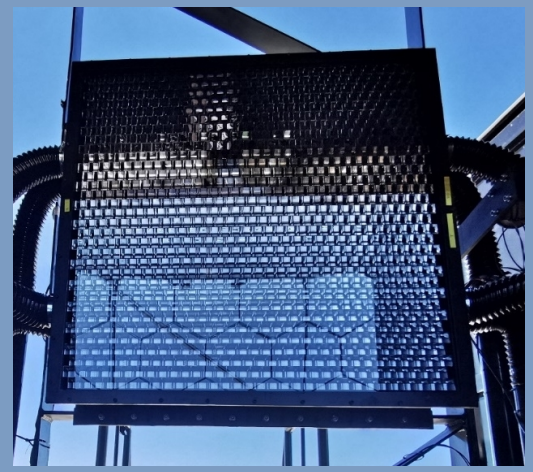

SiPM camera

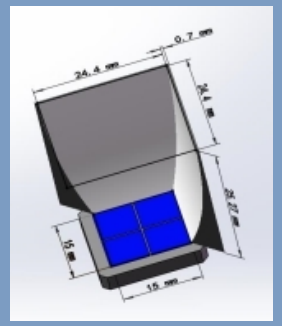

SiPM and Winstone cone

Table 1. LHAASO vs other EAS arrays

Experiment	depth g/cm^2	Detector	ΔE (eV)	e.m. Sensitive Area (m^2)	Instrumented Area (m^2)	Coverage
ARGO-YBJ	606	RPC/hybrid	$3\times10^{11}-10^{16}$	6700	11,000	0.93 (central carpet)
BASJE-MAS	550	scint./muon	$6\cdot10^{12}-3.5\cdot10^{16}$		10^4	
TIBET ASγ	606	scint./burst det.	$5\times10^{13}-10^{17}$	380	3.7×10^4	10^{-2}
CASA-MIA	860	scint./muon	$10^{14}-3.5\cdot10^{16}$	1.6×10^3	2.3×10^5	7×10^{-3}
KASCADE	1020	scint./mu/had	$10^{15}-10^{17}$	5×10^2	4×10^4	
KASCADE -Grande	1020	scint./mu/had	$10^{16}-10^{18}$	370	5×10^5	7×10^{-4}
Tunka	900	open Cher.det.	$3\cdot10^{15}-3\cdot10^{18}$	-	10^6	-
IceTop	680	ice Cher.det.	$10^{15}-10^{18}$	4.2×10^2	10^6	4×10^{-4}
LHAASO	600	Water C scint./mu/had Wide FoV Cher.Tel	$3\times10^{11}-10^{18}$	5.2×10^3	1.3×10^6	4×10^{-3} [KM2A]

Muon detectors

Experiment	m asl	μ Sensitive Area [m^2]	Instrumented Area [m^2]	Coverage
LHAASO	4410	4.2×10^4	10^6	4.4×10^{-2}
TIBET ASγ	4300	4.5×10^3	3.7×10^4	1.2×10^{-1}
KASCADE	110	6×10^2	4×10^4	1.5×10^{-2}
CASA-MIA	1450	2.5×10^3	2.3×10^5	1.1×10^{-2}

如何探测宇宙线线?

每天收集10多亿高能宇宙线/伽马射线引发粒子“阵雨”

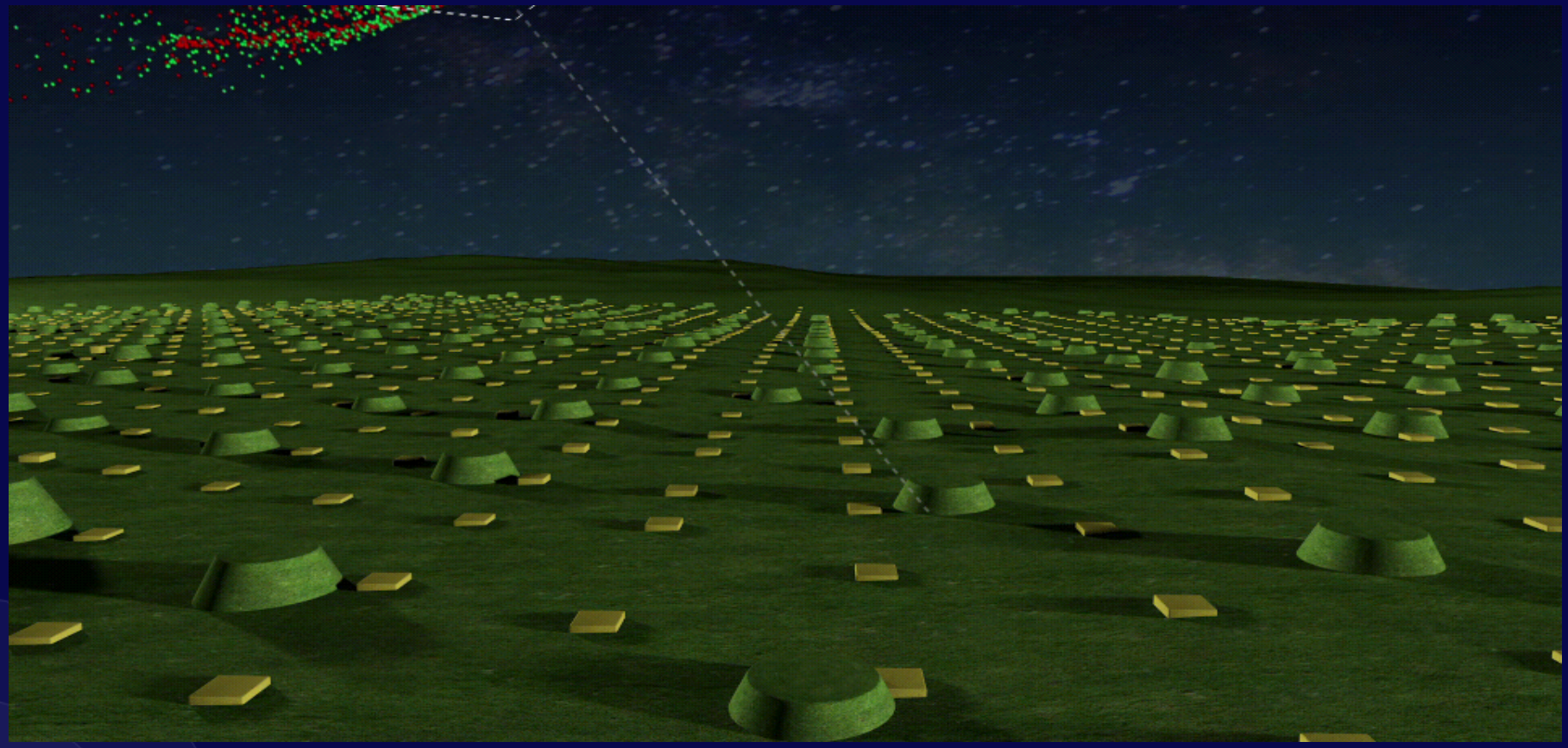

“阵雨”洒落在“拉索”阵列上，一场“雨”持续的时间只有几十微秒

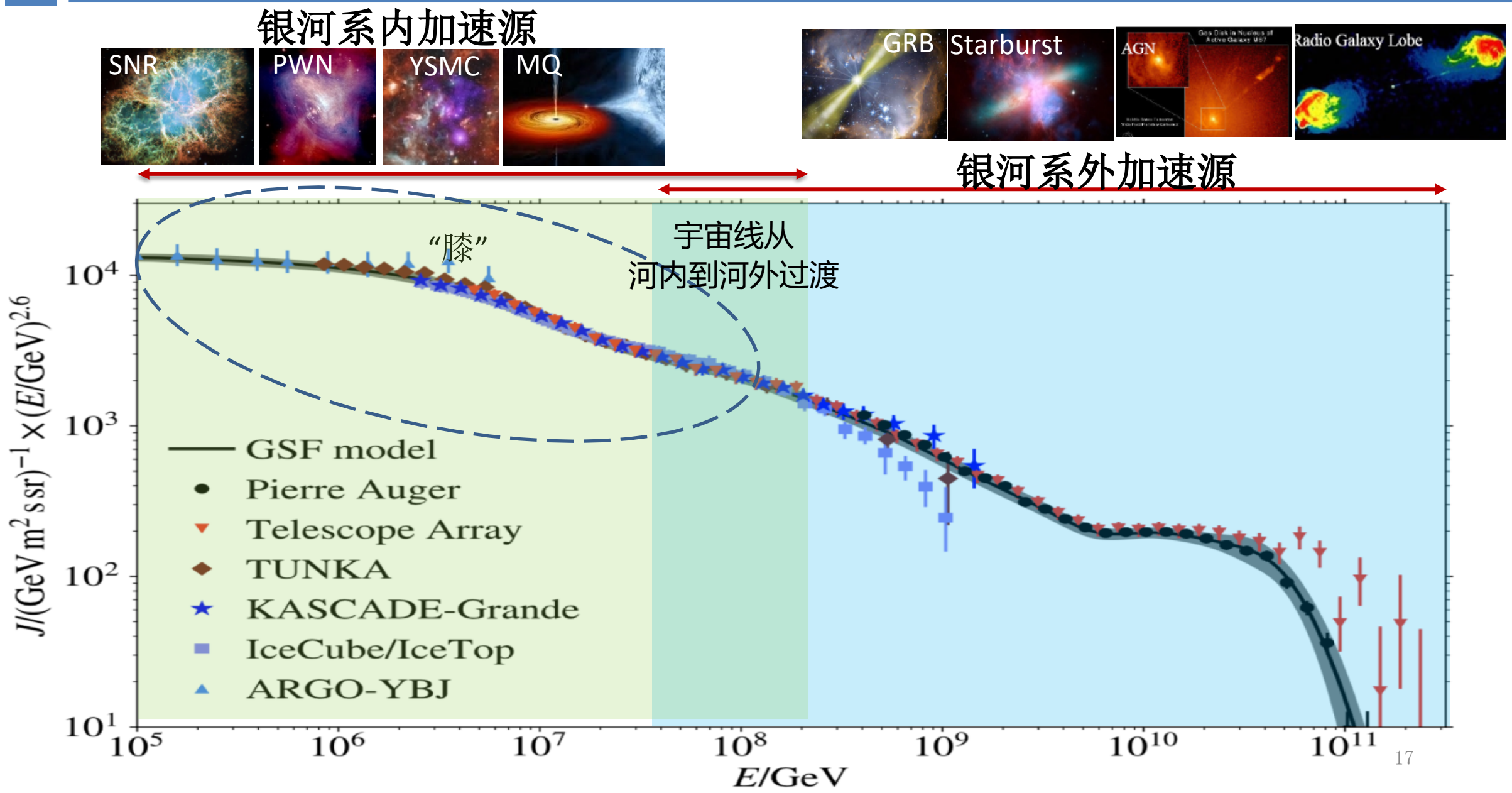
银河系内加速源
SNR
PWN
YSMC
MQ
GRB
Starburst
AGN
Radio Galaxy Lobe
银河系外加速源
“膝”
宇宙线从
河内到河外过渡
GSF model
Pierre Auger
Telescope Array
TUNKA
KASCADE-Grande
IceCube/IceTop
ARGO-YBJ
$J/(\mathrm{GeV\,m^2\,s\,sr})^{-1} \times (E/\mathrm{GeV})^{2.6}$
10^4
10^3
10^2
10^1
10^5
10^6
10^7
10^8
10^9
10^{10}
10^{11}
E/GeV

如何探测宇宙线线?

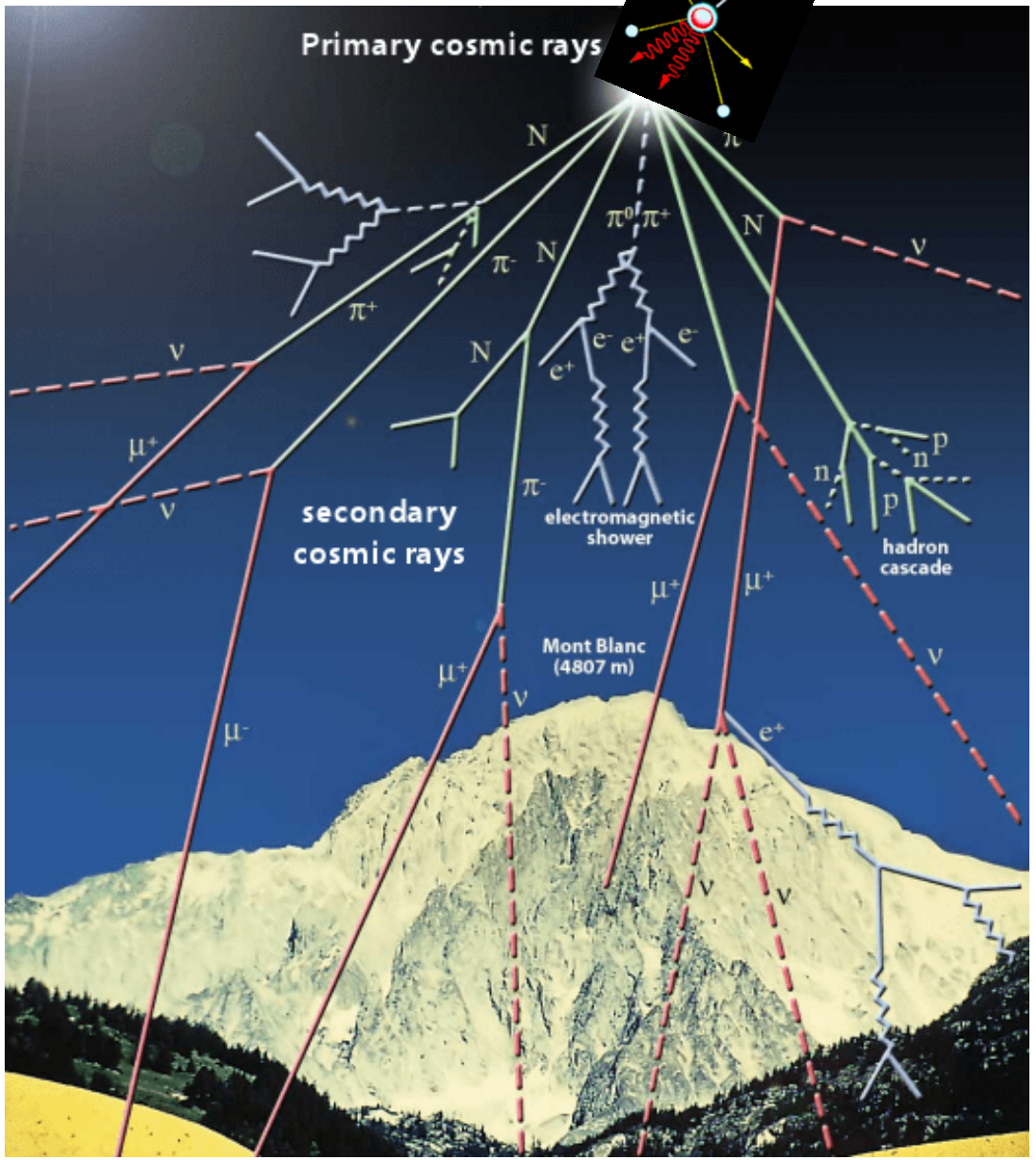

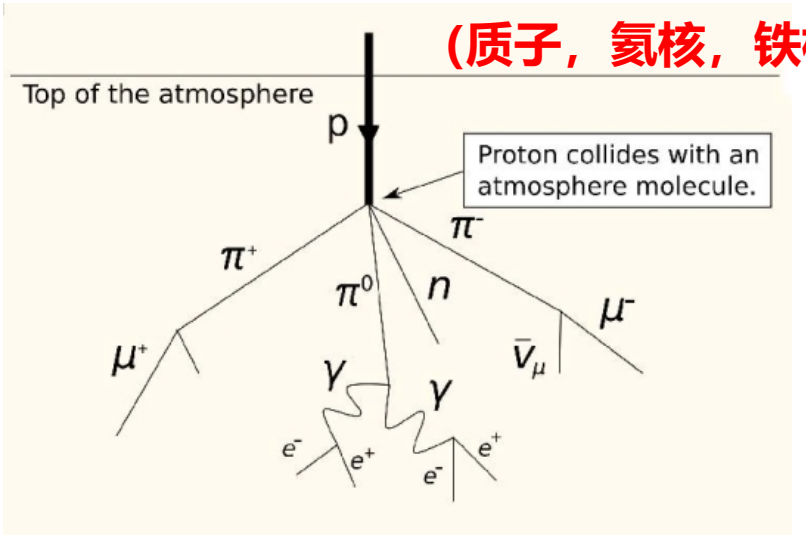

（质子，氦核，铁核等核子）

Development of gamma–ray air showers

伽马光子

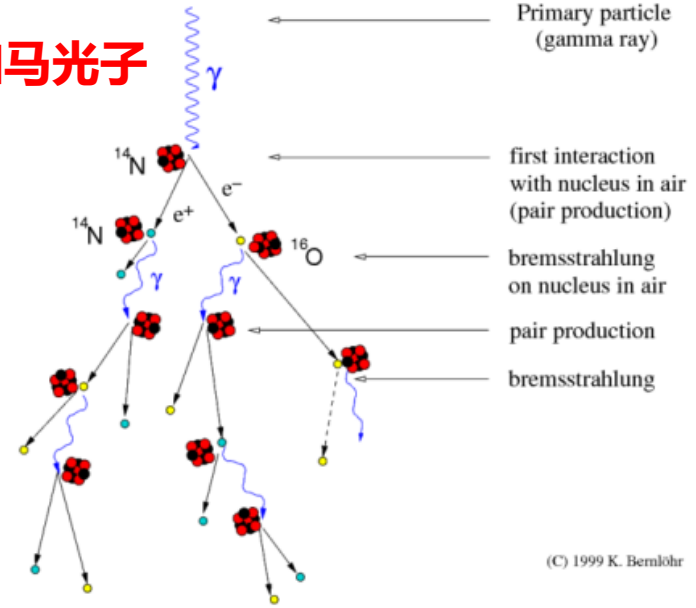

次级粒子：

正负电子、

伽马光子、

强子、

μ子、

中微子、

荧光、

Cherenkov光。

Soft interaction models

Collider based

- PYTHIA (瑞典)
  - 以弦模型为基础多重产生维像模型
  - arXiv:1101.2599 review
- DPMJET （法国人）
  - Dual Parton Model

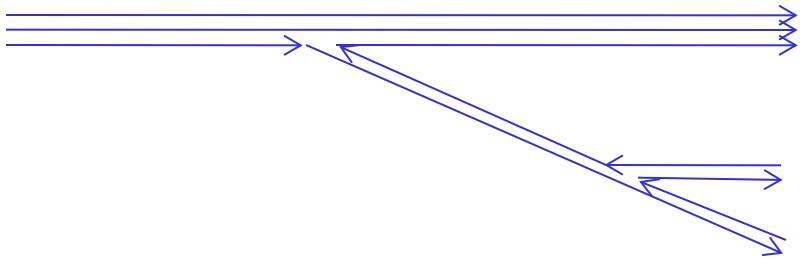

  - arXiv:hep-ph/0012252

Cosmic ray researches

- QGSJET （俄国）
  - QCD **pomeron** (Regge Pole theory) model

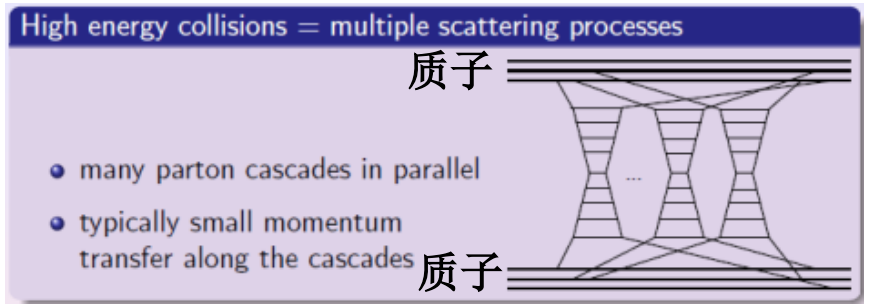

[SO, PLB636 (2006) 40; PRD77 (2008) 034009; PRD83 (2011) 014018]

- SIBYLL
  - Mini-Jet Model, parton cascading in both structure and fragmentation, Q^2-dependence
- EPOS (next page)

LHCf Experimental Set-up

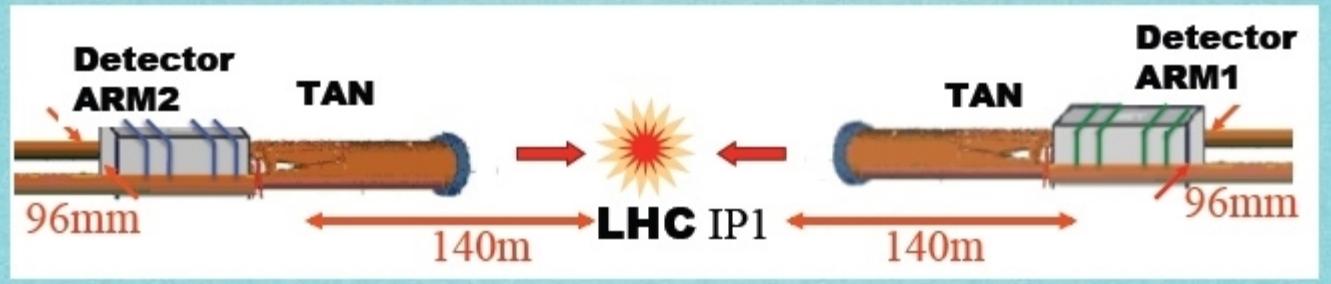

Detectors installed in the TAN region, 140 m away from ATLAS Interaction Point (IP1)

- Here the beam pipe splits in 2 separate tubes.
- Charged particle are swept away by magnets
- We will cover up to $y \to \infty$

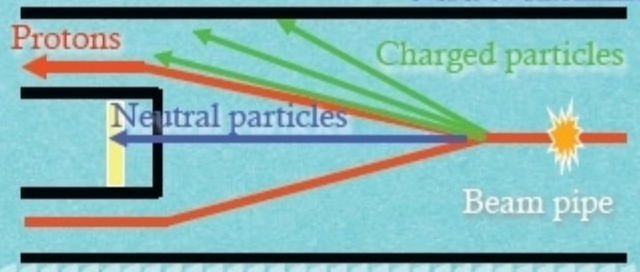

Alessia Tricomi
University & INFN Catania

experiment at LHC
, 2010, Paris

LHCf experiment

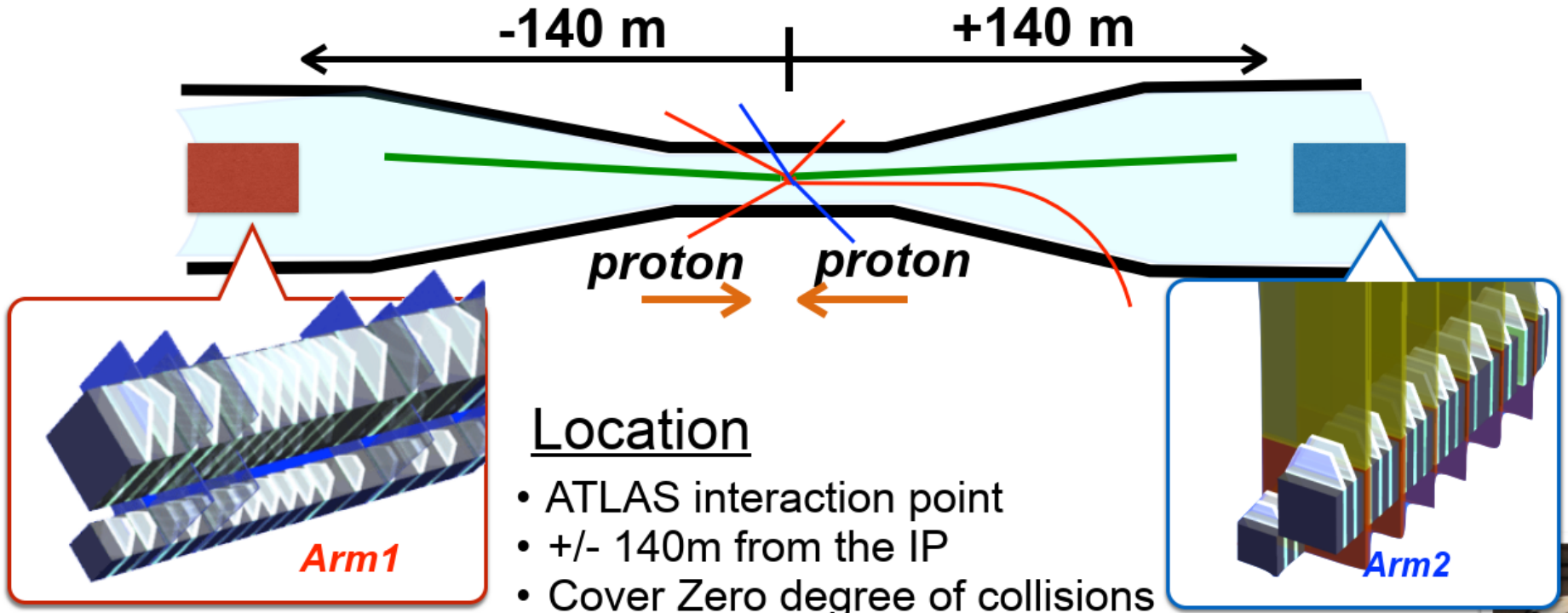

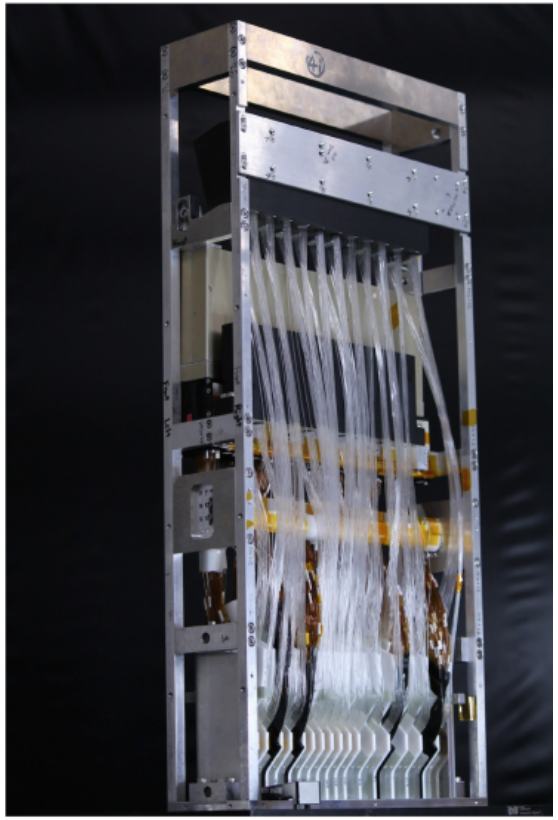

Location

- ATLAS interaction point
- +/- 140m from the IP
- Cover Zero degree of collisions pseudo rapidity η > 8.4

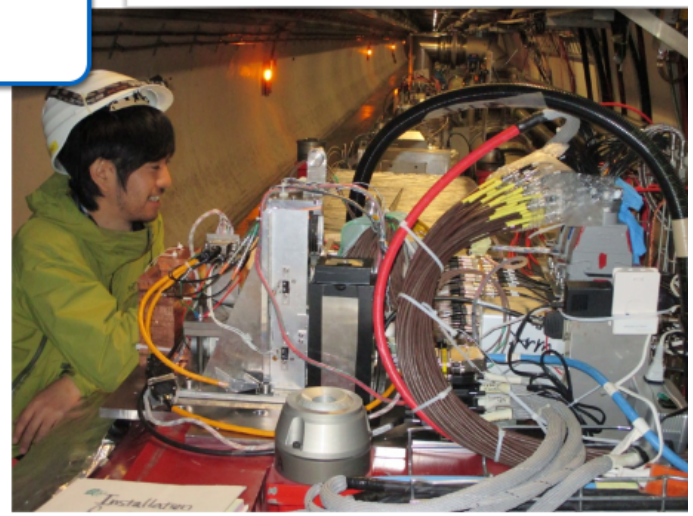

LHCf detectors

- Sampling and positioning calorimeters
- Two towers, 20x20, 40x40mm^2 (Arm1) , 25x25, 32x32mm^2(Arm2)
- Tungsten layers, 16 GSO scintillators, 4 position sensitive layers (Arm1: GSO bar hodoscopes, Arm2: Silicon strip detectors)
- Thickness: 44 r.l. and 1.7 λ

DPMJET 3.04 QGSJET II-03 SIBYLL 2.1 EPOS 1.99 PYTHIA 8.145

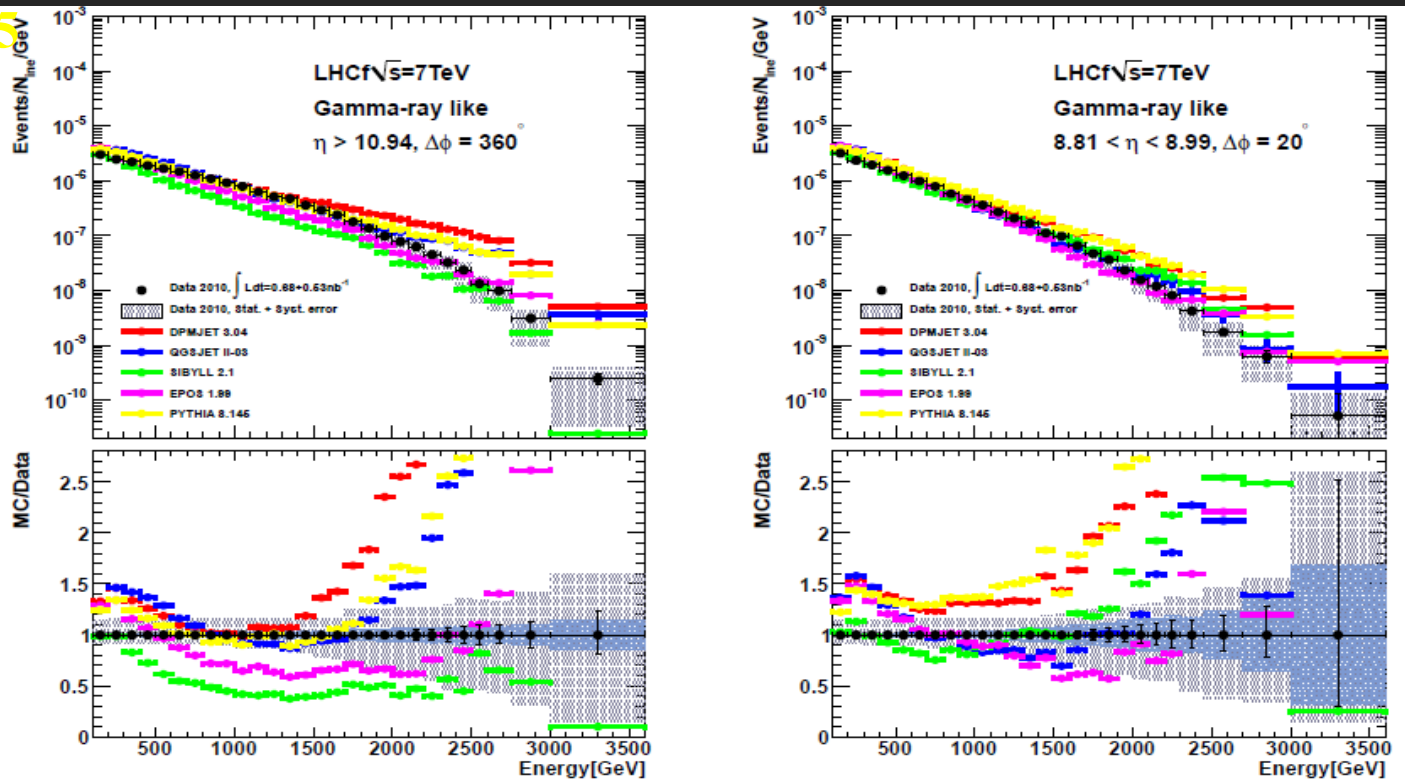

1. None of the models perfectly agree with data.
2. QGSJET II, DPMJET3, PYTHIA8: good agreement in 0.5-1.5TeV at $\eta>10.94$ but large difference >2TeV.
3. SIBYLL2 shows good spectral shape >0.5TeV at $\eta>10.94$ but only half yield
4. Less deviation at $8.81<\eta<8.99$ but still big difference >2TeV in DPMJET3 and PYTHIA8

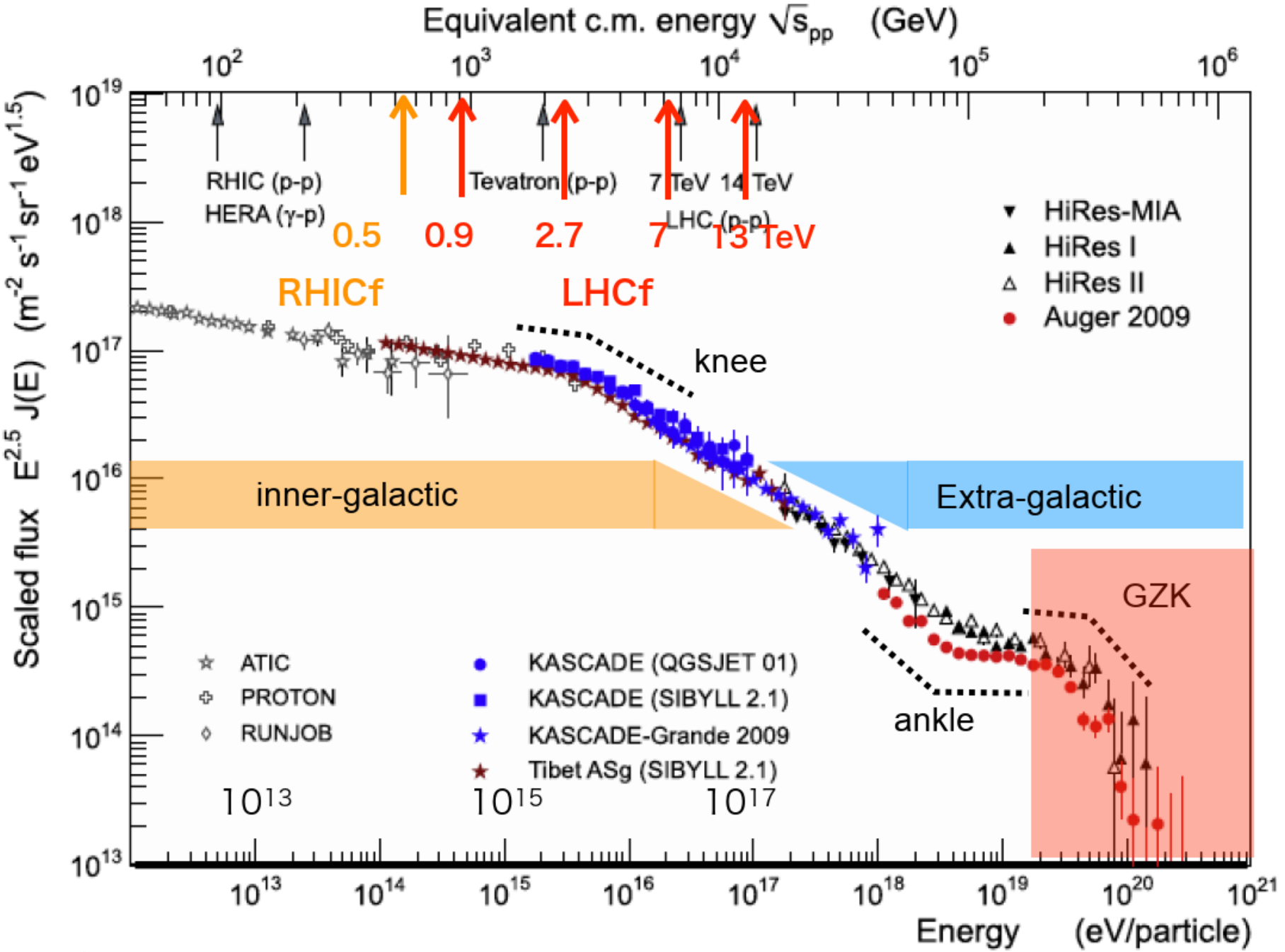
Equivalent c.m. energy $\sqrt{s_{pp}}$ (GeV)
10^2
10^3
10^4
10^5
10^6
RHIC (p-p)
HERA (γ-p)
Tevatron (p-p)
7 TeV
14 TeV
LHC (p-p)
0.5
0.9
2.7
7
13 TeV
RHICf
LHCf
HiRes-MIA
HiRes I
HiRes II
Auger 2009
knee
inner-galactic
Extra-galactic
GZK
ankle
ATIC
PROTON
RUNJOB
KASCADE (QGSJET 01)
KASCADE (SIBYLL 2.1)
KASCADE-Grande 2009
Tibet ASg (SIBYLL 2.1)
10^{13}
10^{15}
10^{17}
Scaled flux $E^{2.5}$ J(E) $(m^{-2}\ s^{-1}\ sr^{-1}\ eV^{1.5})$
10^{19}
10^{18}
10^{17}
10^{16}
10^{15}
10^{14}
10^{13}
10^{13}
10^{14}
10^{15}
10^{16}
10^{17}
10^{18}
10^{19}
10^{20}
10^{21}
Energy (eV/particle)

Energy dependency of muon deficit

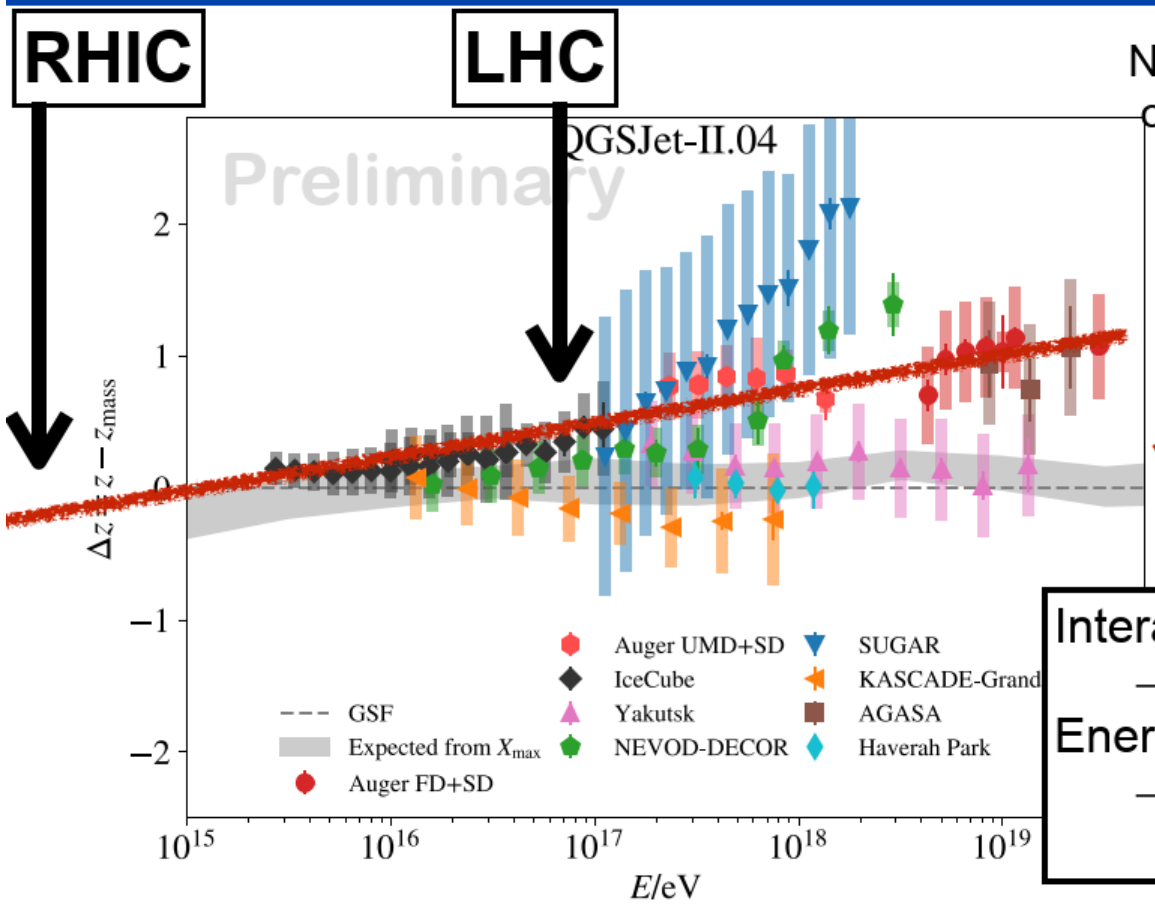

Normalized muon numbers results observed by several CR experiments

$$z = \frac{\ln(N_\mu^{\rm det}) - \ln(N_{\mu p}^{\rm det})}{\ln(N_{\mu \rm Fe}^{\rm det}) - \ln(N_{\mu p}^{\rm det})}$$

Muon deficit

$$z_{\rm mass} \approx \frac{\langle \ln A \rangle}{\ln 56}$$

Interaction study at the highest energy
→ LHC ($\sqrt{s}$=14TeV, $E_{\rm lab} = 10^{17}$eV)
Energy dependency
→ RHIC ($\sqrt{s}$=0.5 TeV, $E_{\rm lab} = 10^{14}$eV) v.s. LHC

J.C. Arteaga-Velmázquez ICRC2023

Blurry Picture.

- "Muon Puzzle" (<N_μ>) depends on energy measurement technique
  - Update of WHISP analysis (2023)

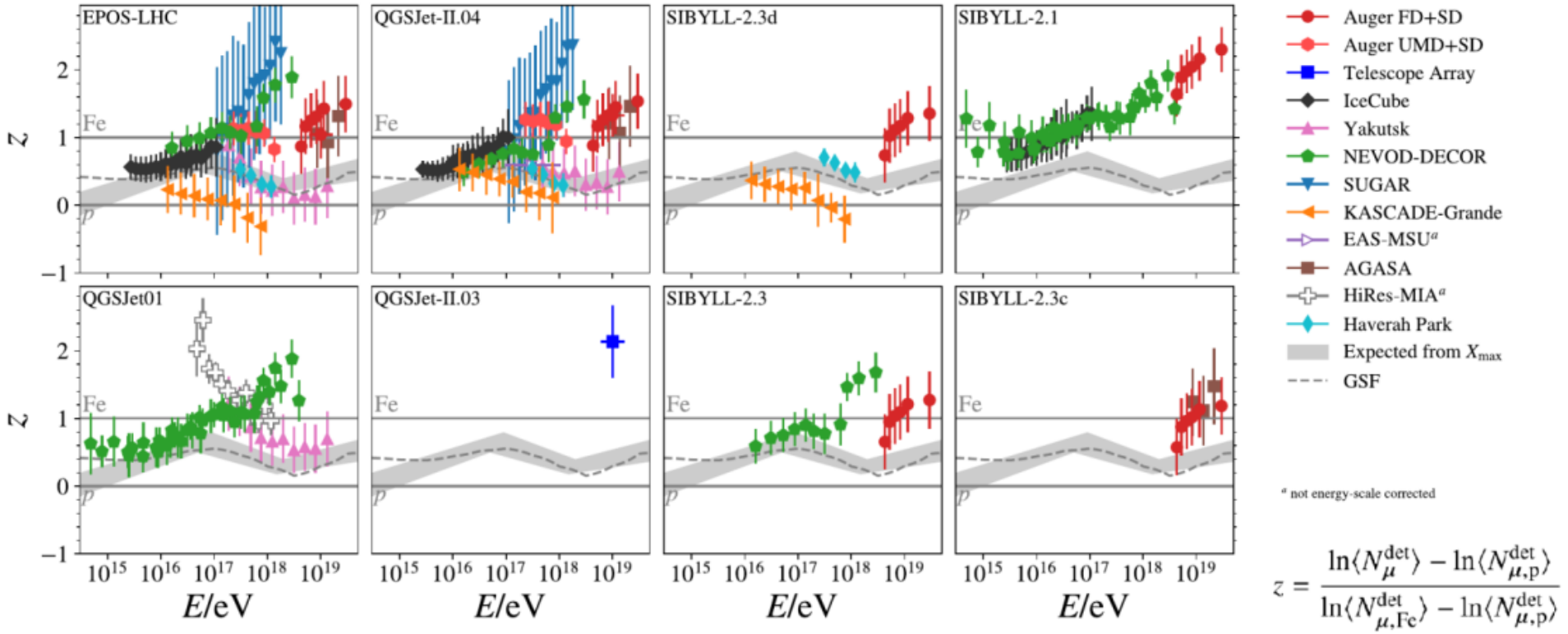

J.C. Arteaga-Update on the combined analysis of μ data ICRC 2023, Nagoya, Japan 11

Muon content

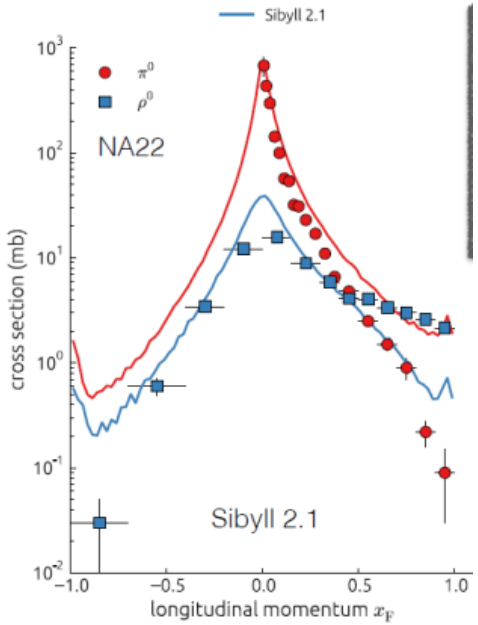

$x_p = p_{||}/p_{max}$

- **Very unstable in models:**
  - **Tiny change in ρ^0–production as a leading particle in π–p colliding**
  - **Huge difference in muon content**

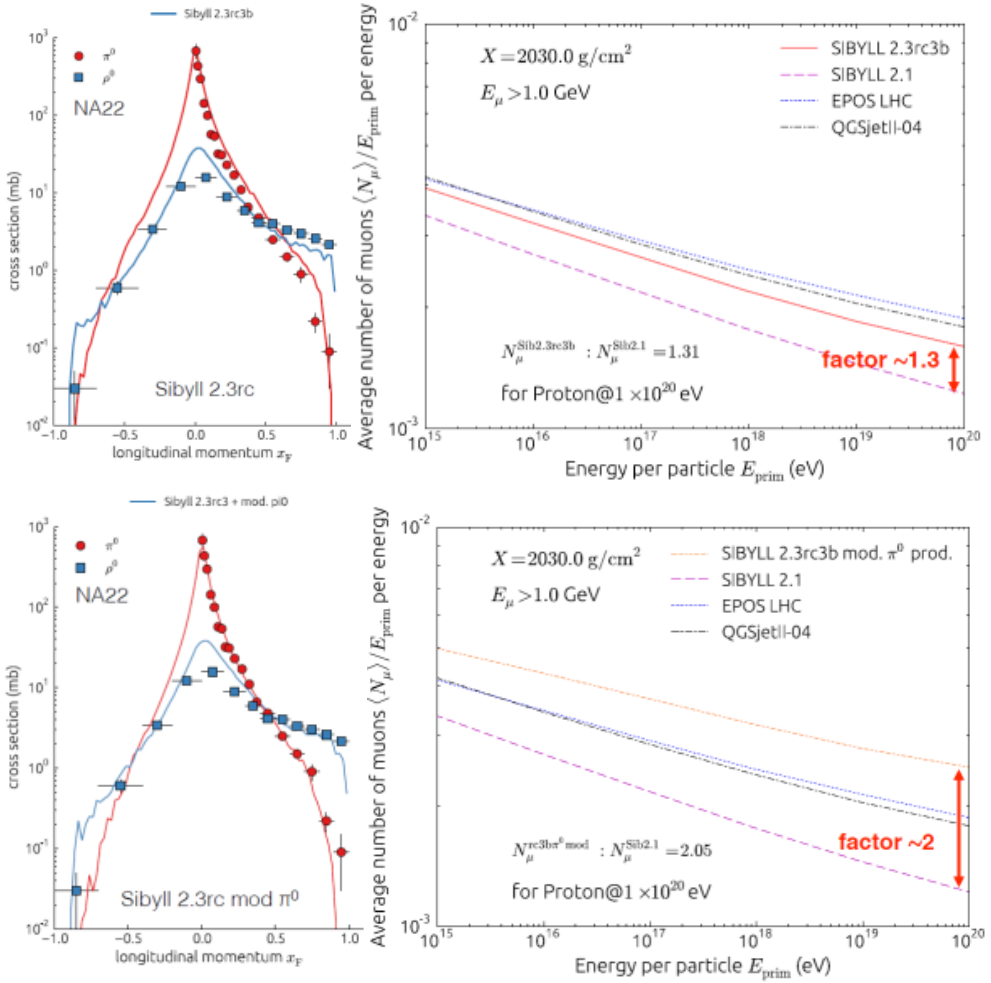

Riehn *et al.*, ICRC 2015

X_{max} and N_μ

Global changes

- Taking into account new data, new EPOS shifted by +20g/cm² (+/- 5g/cm²)
- QGSJETIII-01 shifted by +15g/cm² (=EPOS LHC)
- Increase of the number of muons by about 10% (+/- 5%) for EPOS LHC-R

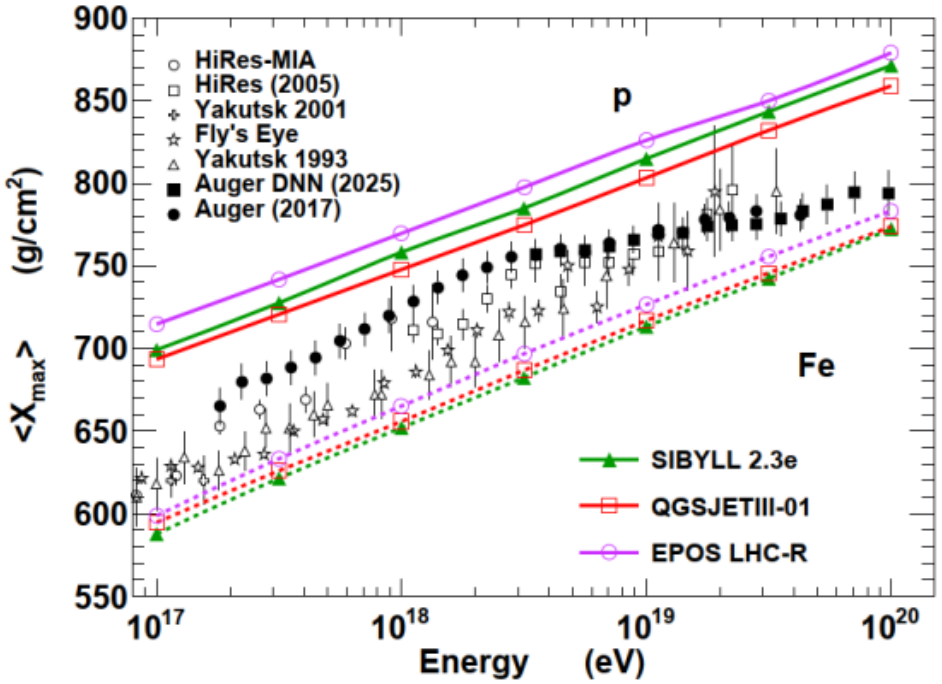

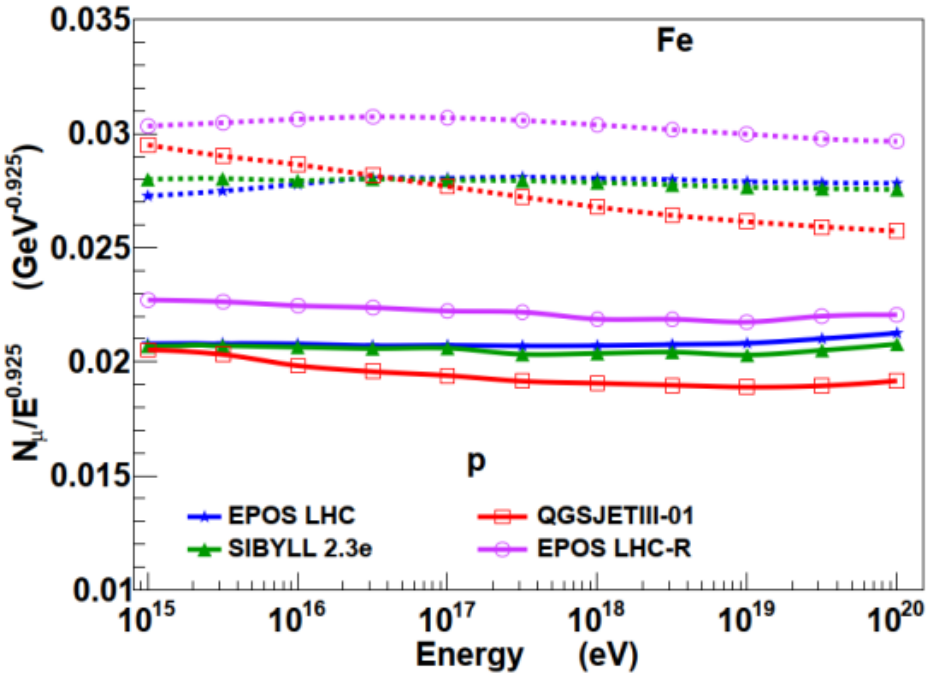

27

Pseudorapidity

Simple (basic) measurement still important !

- **New data at 13 TeV in p-p**
  - Test extrapolation with different triggers
  - Sibyll has a clear difference with other models (and data) : too narrow !
- Detailed data at 5 TeV for p-Pb

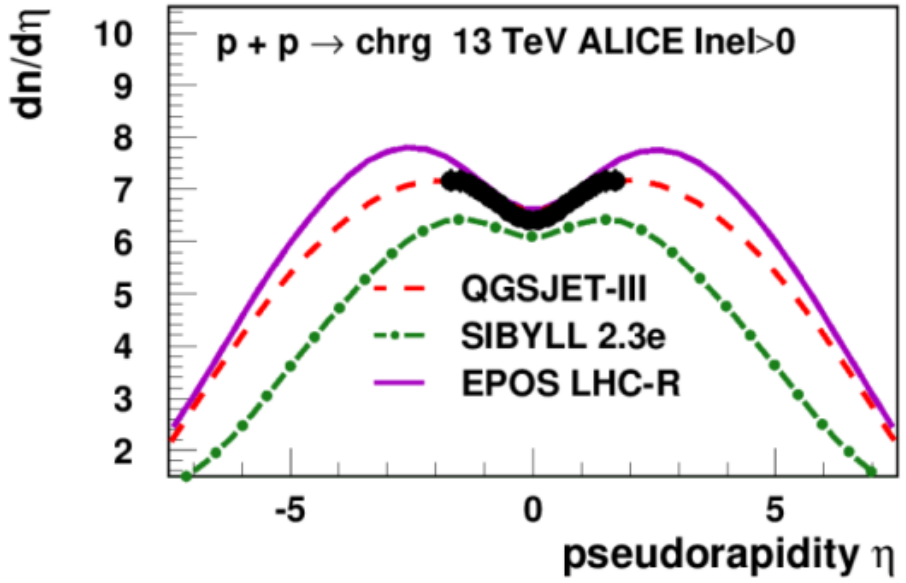

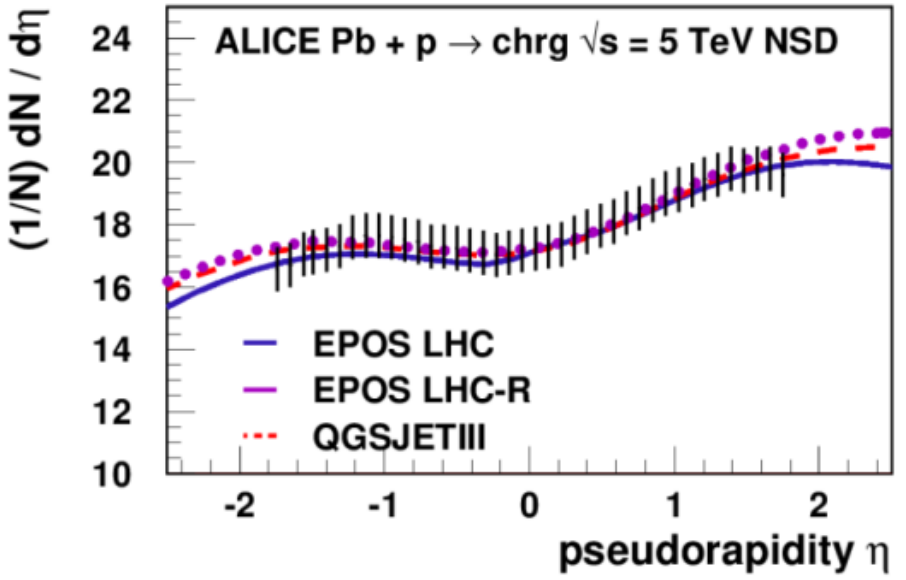

"Muon Puzzle"

EPOS LHC-R, first model producing a deeper X_{max} and more muons and being compatible with all measured accelerator data :

- Deeper X_{max} give larger <lnA> reducing the gap with measured muon content
- Increase of muons further decrease the gap to reach Auger systematics
- No big change for QGSJETIII
  - Impact at low energy ???

$$z = \frac{\ln N_{\mu}^{\det} - \ln N_{\mu,p}^{\det}}{\ln N_{\mu,\mathrm{Fe}}^{\det} - \ln N_{\mu,p}^{\det}}$$

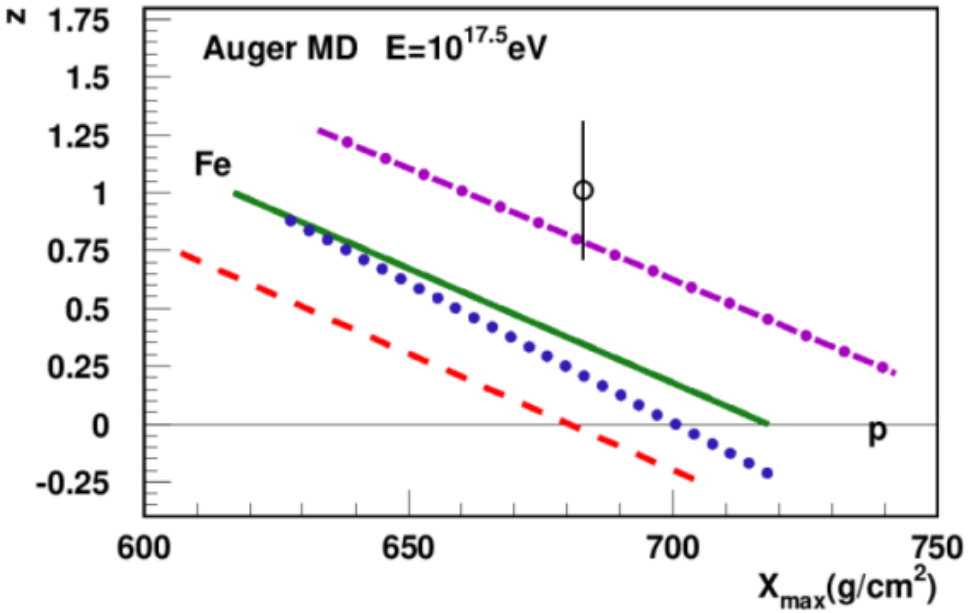

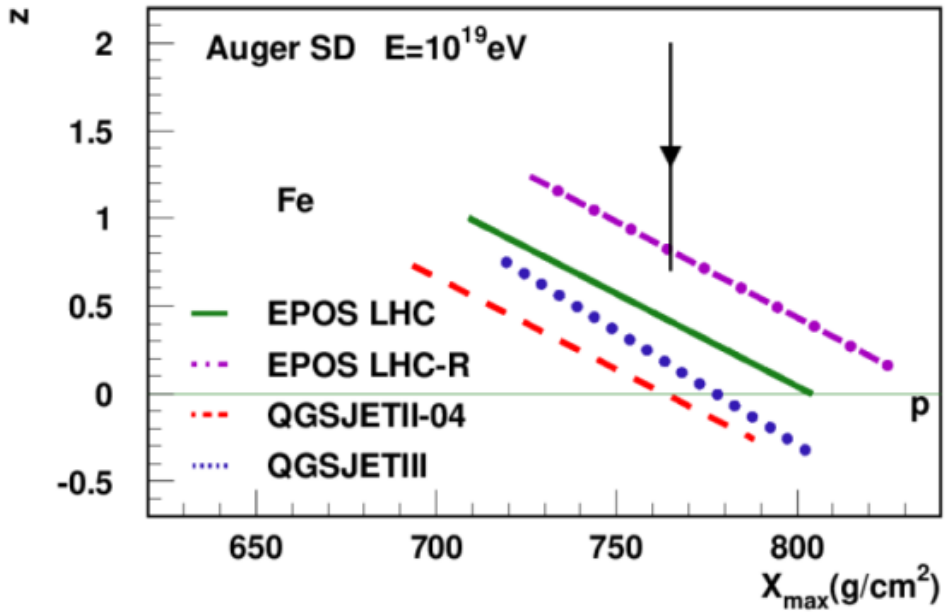

$$P_{\mu e} = \log_{10} \frac{N_\mu}{N_e^{0.82}}$$

$$P_{\theta c} = \frac{\theta_c^{250} - \langle \theta_c^{250} \rangle}{\langle \theta_c^{250} \rangle|_{PeV}}$$

和Xmax相关

- N_μ: 40~200 m
- N_e: 40~200 m

$$P_{\theta c+\mu e} = -\sin(\delta) \cdot P_{\theta c} + \cos(\delta) \cdot P_{\mu e}$$

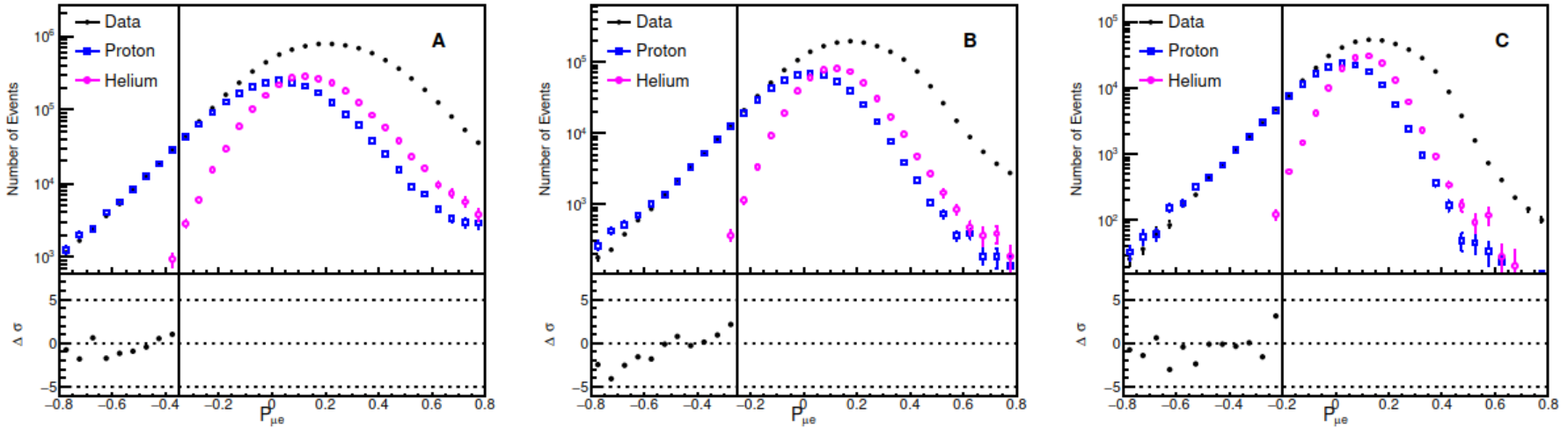

Figure S16: **Parameter comparison.** These three sets of figures represent the comparisons of $P_{\theta c+\mu e}$ in the energy ranges of $10^{5.2} \sim 10^{5.6}$ GeV (pad A), $10^{5.6} \sim 10^{6.0}$ GeV (pad B), and $10^{6.0} \sim 10^{7.1}$ GeV (pad C). The above row shows the distribution of $P_{\theta c+\mu e}$ in both the data and the simulation in different energy intervals. The simulation events are based on EPOS-LHC model. The black dots represent the data, while the blue square represent proton events in simulation and pink circle represent Helium events in simulation. The row below shows the deviation between the data and the simulation.

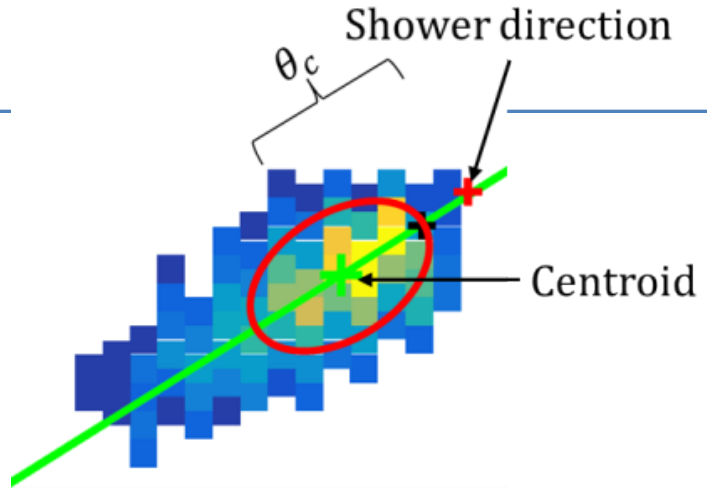

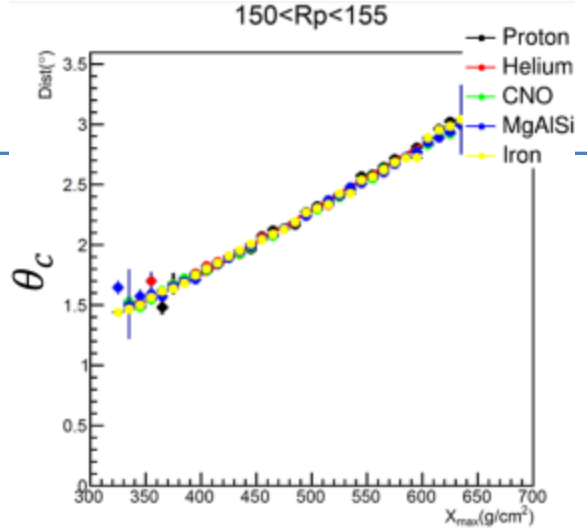

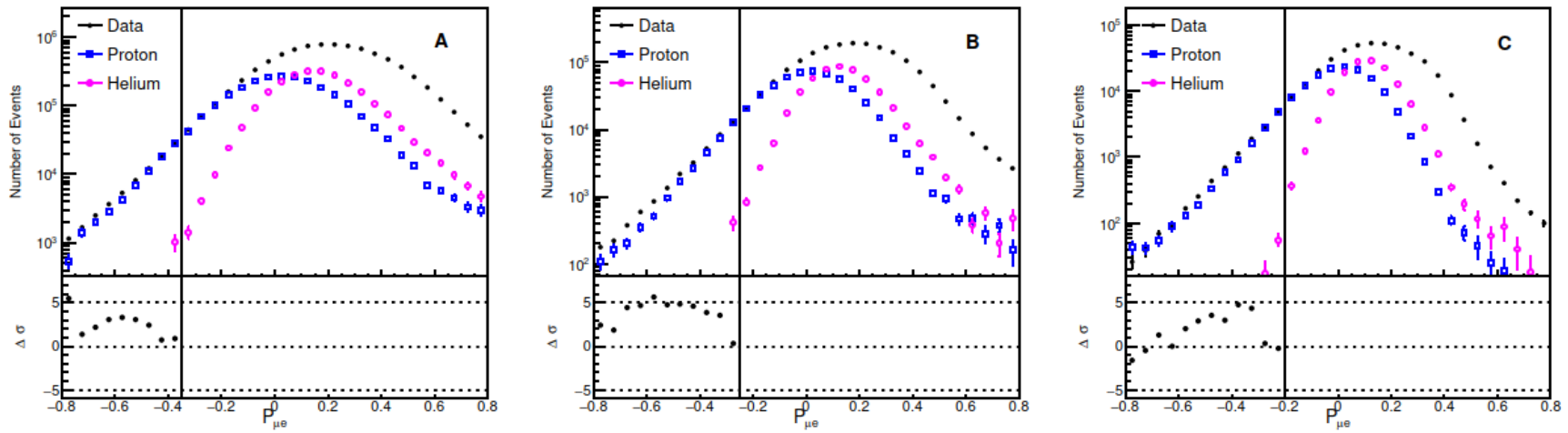

Figure S17: **Parameter comparison.** These three sets of figures represent the comparisons of $P_{\theta c+\mu e}$ in the energy ranges of $10^{5.2} \sim 10^{5.6}$ GeV (pad A), $10^{5.6} \sim 10^{6.0}$ GeV (pad B), and $10^{6.0} \sim 10^{7.1}$ GeV (pad C). The above row shows the distribution of $P_{\theta c+\mu e}$ in both the data and the simulation in different energy intervals. The simulation events are based on QGSJET model. The black dots represent the data, while the blue square represent proton events in simulation and pink circle represent Helium events in simulation. The row below shows the deviation between the data and the simulation.

Proton Selection

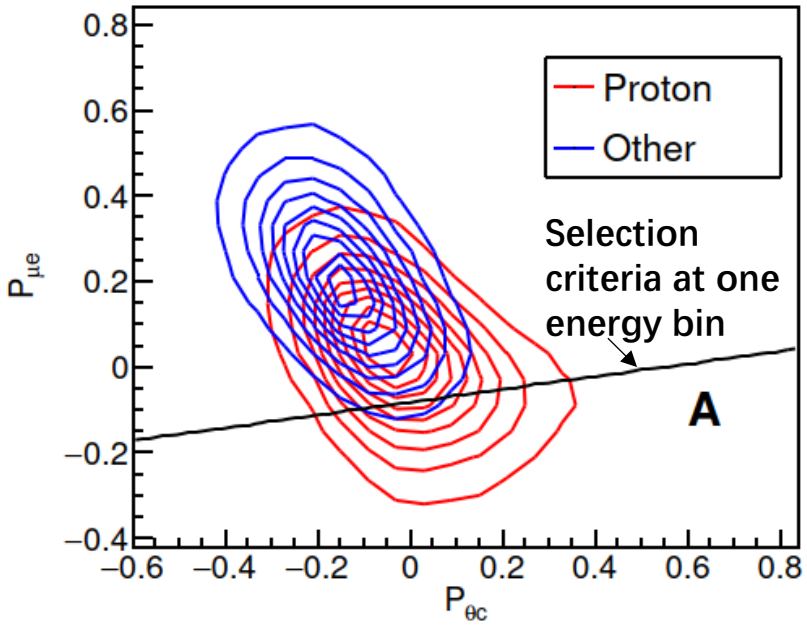

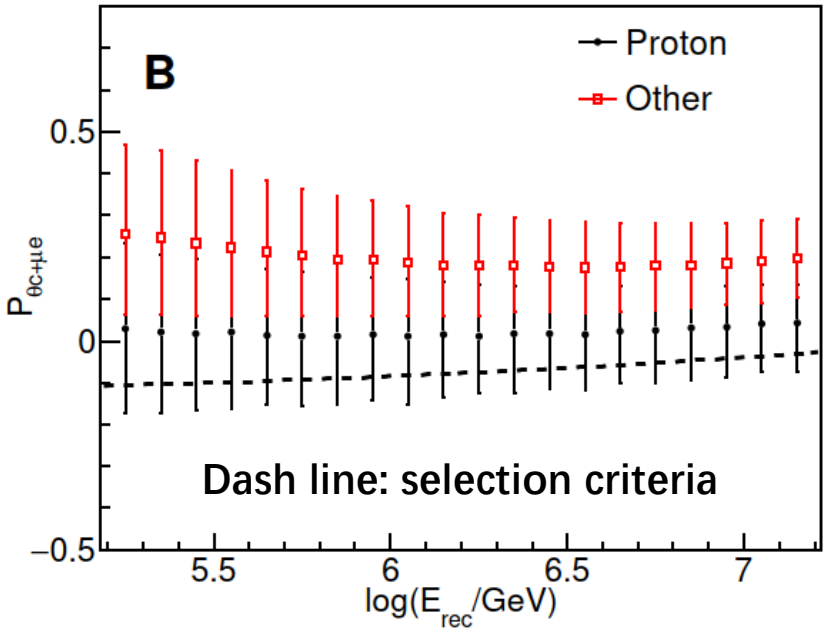

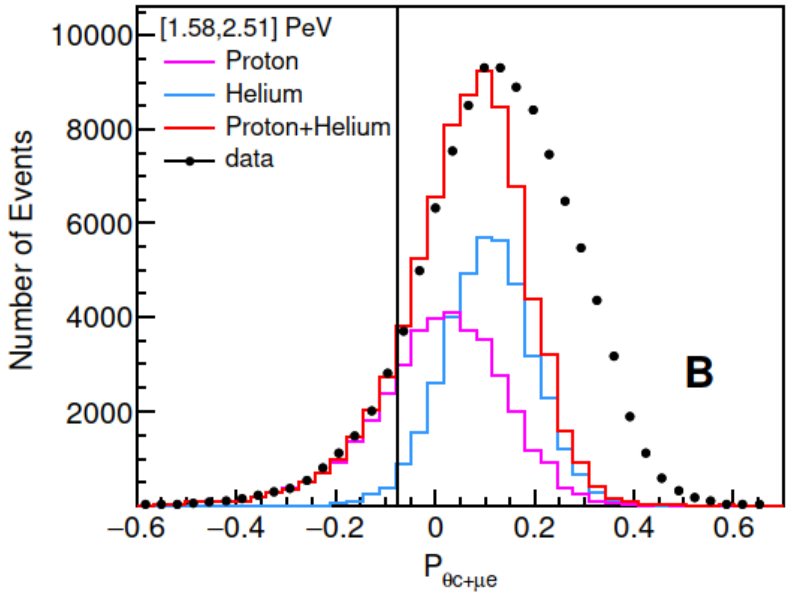

$$P_{\theta c+\mu e} = -\sin(\delta)\cdot P_{\theta c} + \cos(\delta)\cdot P_{\mu e} \quad (\delta = 8.5^\circ)$$

- Purity ($\epsilon^l = \frac{N^L_{select}}{N^L_{select}+N^H_{select}}$) : ~90% @ 1PeV
  - Most of the contaminations come from Helium
- Selection efficiency ($\eta^l = \frac{N^L_{select}}{N^L_{all}}$) : 25%.

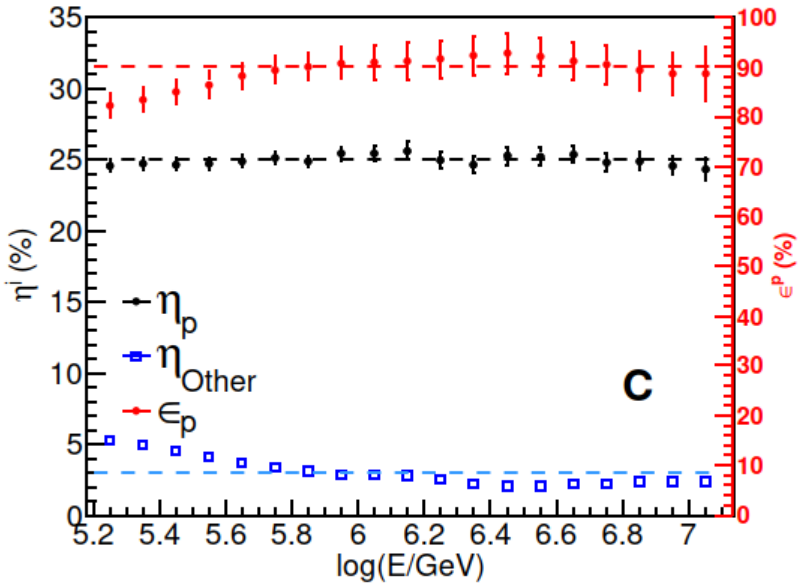

Energy Reconstruction

- Electromagnetic component : Cherenkov photons (N_{ph}) or electrons + gamma rays (N_e)
- *Hadronic component*: $\pi^{\pm} \rightarrow \mu$ （ N_μ ）

$$N_{c\mu} = N_{ph} + CN_u$$
$$E_{rec} = kN_{c\mu}$$

- Energy Resolution : <15%
- Systematic Bias : <2%

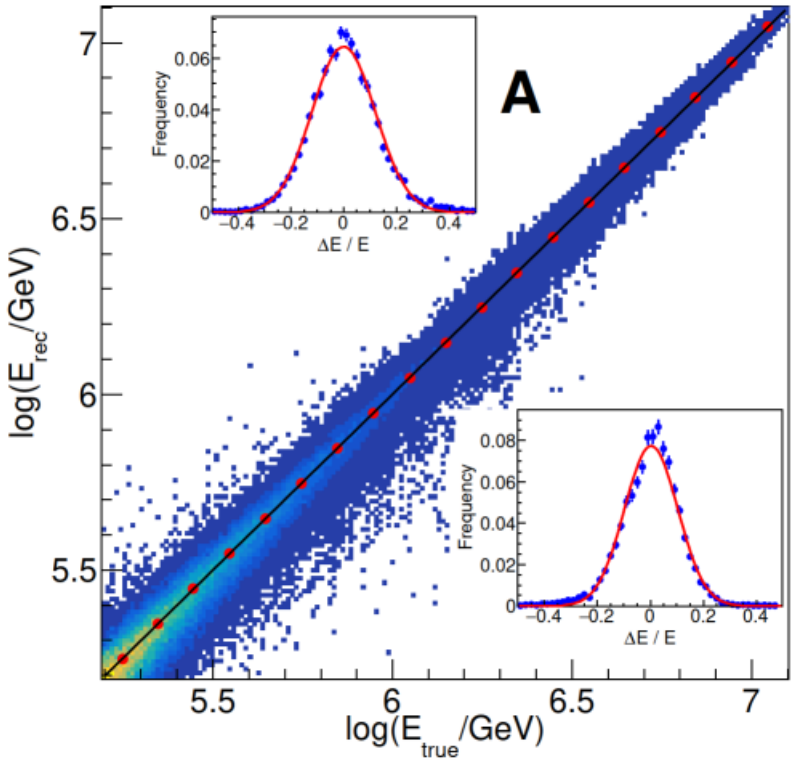

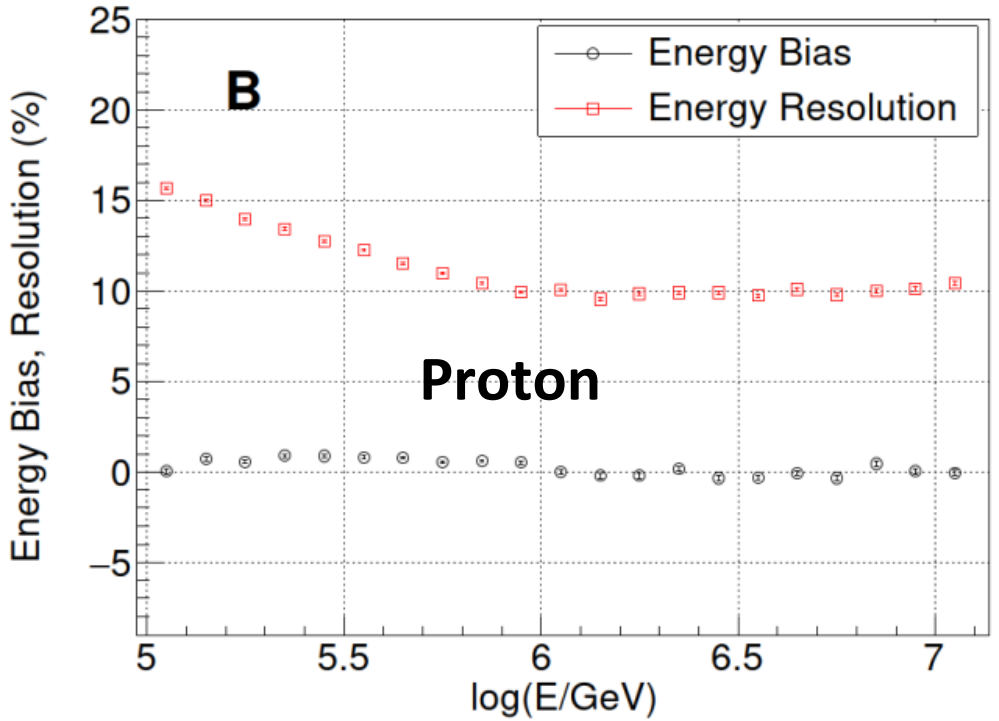

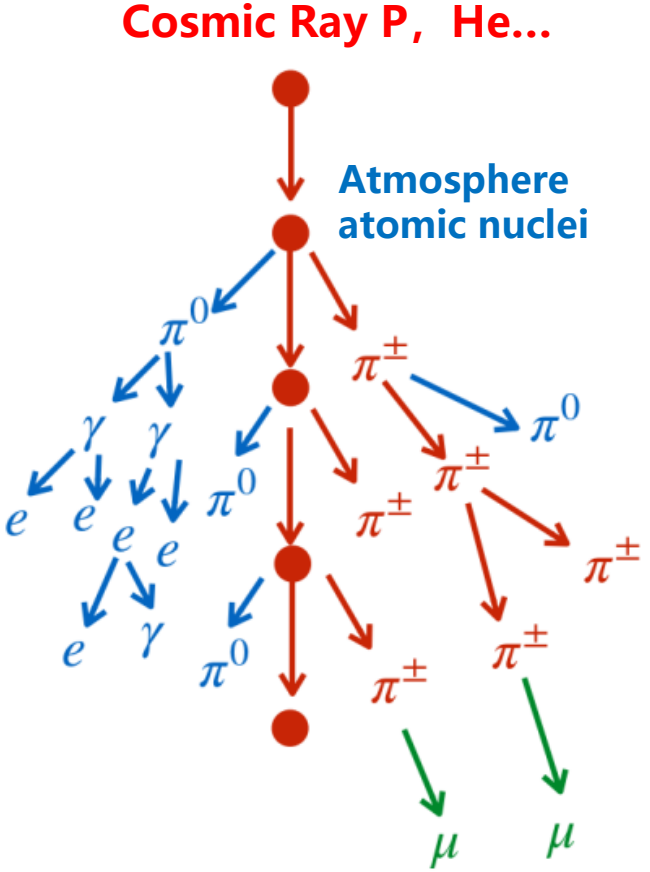

Energy reconstruction

- Energy reconstruction independent of the primary CR component
- Scintillator detector array（ED）： Electromagnetic component （N_e ）
- Muon detector array （MD）： *hadron component* $\pi^{\pm} \rightarrow \mu$ （ N_μ ）

$$N_{e\mu} = N_e + aN_\mu \qquad E_{rec} = b \times N_{e\mu}$$

J. Matthews, Astropart. Phys. 22, 387 (2005)

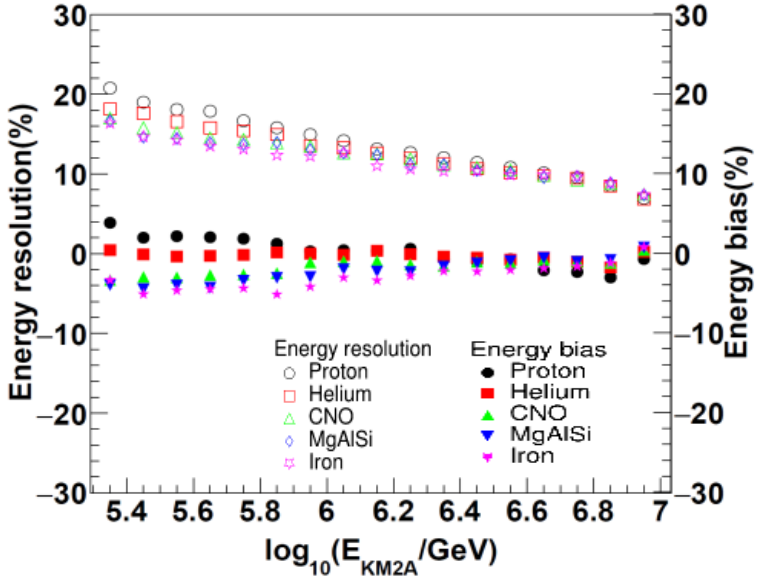

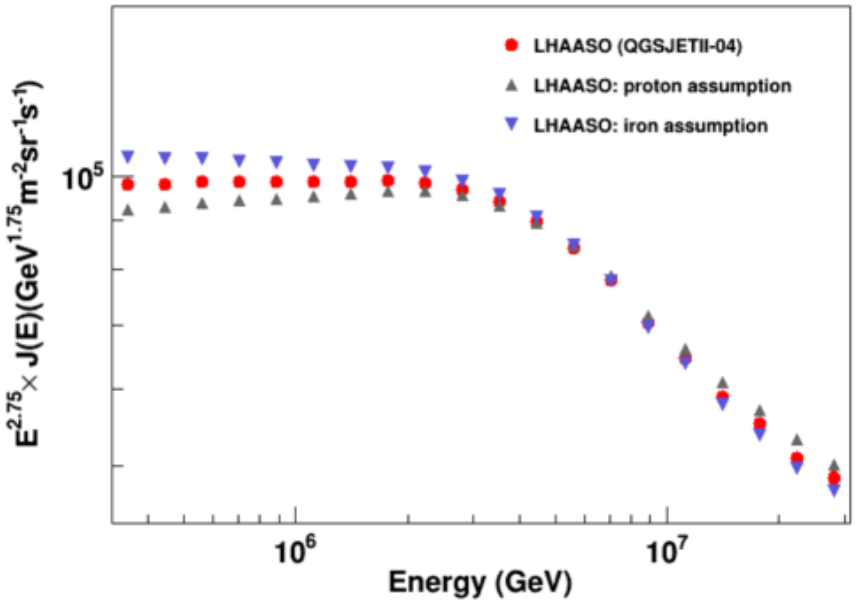

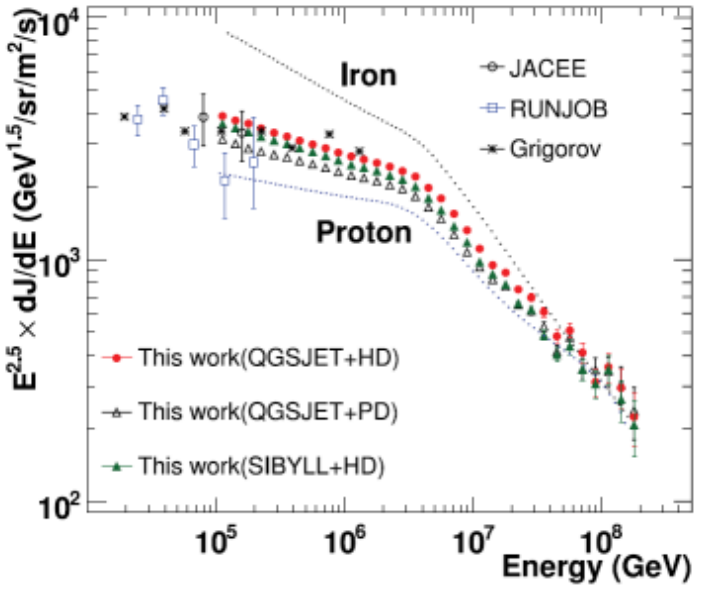

PHYSICAL REVIEW D 106, 123028 (2022)

All-particle energy spectrum & composition by LHAASO

(from 0.3 to 30 PeV)

LHAASO Collaboration, PHYSICAL REVIEW LETTERS 132, 131002 (2024)

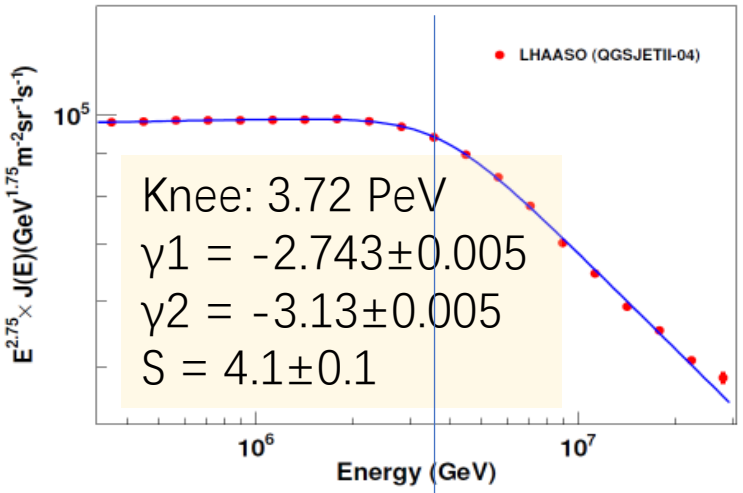

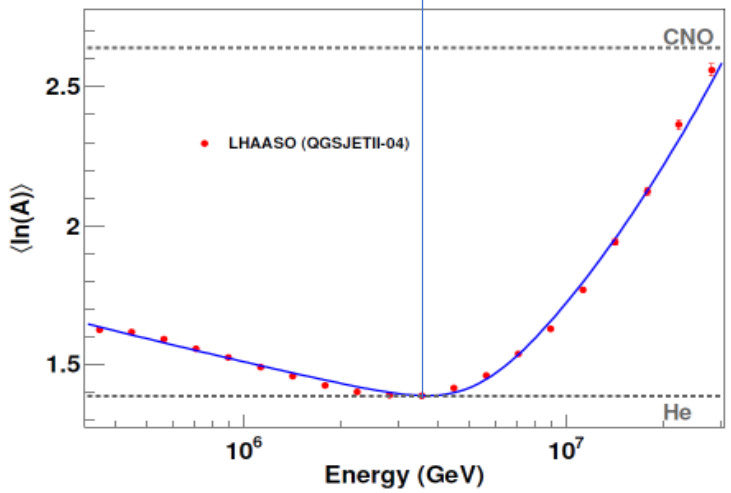

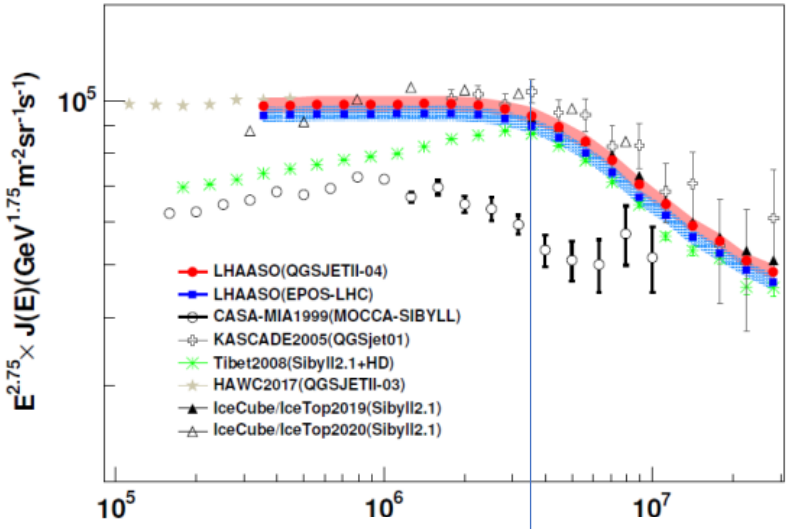

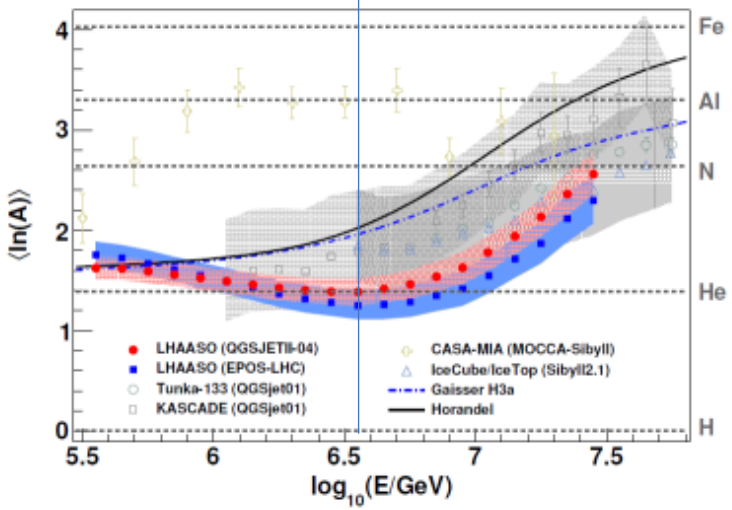

- Systematic uncertainties are sufficiently small
- This unveils a clear correlation between the flux and the composition at the knee

总结和展望

- LHAASO于2019年4月1/4阵列投入运行，2021年7月全阵列建成，2023年5月通过国家验收
- 2021年在银河系内发现了12个超高能伽马射线源，至2023年，数量增加至43个
  - 揭示了银河系内普遍存在拍电子伏超高能伽马射线源
  - 几乎涵盖银河系内所有的高能天体：超新星遗迹、脉冲星脉、脉冲星风云、大质量星团等
  - LHAASO打开了前沿学科“超高能伽马天文学”新窗口
- LHAASO最精确测量了宇宙线全粒子能谱和平均质量
- 宇宙线“膝区” 质子能谱、轻成分能谱、氦核能谱即将发布
- 宇宙线大气簇射物理研究
  - 高能强相互作用模型
  - 簇射中的缪子数
  - …
- 寻找新物理：新粒子、暗物质?
- AI 应用于粒子鉴别

新物理探索：洛伦兹对称性破缺研究

- Using the most energetic γ-rays observed by LHAASO
  - The Lorentz symmetry was tested for the 1st order effect w/ the breaking energy 10^5 higher than the Planck scale, a dozen of times higher than the previous result
  - The 2nd order effect is still possible, w/ the breaking energy 10^3 below the Planck scale

Process: $\gamma \rightarrow e^+e^-$

$$E^{(1)}_{\rm LIV} \gtrsim 9.57\times10^{23}\ {\rm eV}\left(\frac{E_\gamma}{\rm TeV}\right)^3,$$

$$E^{(2)}_{\rm LIV} \gtrsim 9.78\times10^{17}\ {\rm eV}\left(\frac{E_\gamma}{\rm TeV}\right)^2.$$

Process: $\gamma \rightarrow 3\gamma$

$$\Gamma_{\gamma\to3\gamma} = 5\times10^{-14}\frac{E_\gamma^{19}}{m_e^8 E^{(2)10}_{LIV}},$$

$$E^{(2)}_{LIV} > 3.33\times10^{19}{\rm eV}\left(\frac{L}{\rm kpc}\right)^{0.1}\left(\frac{E_\gamma}{\rm TeV}\right)^{1.9}.$$

Source	L (kpc)	$E_{\rm max}$ (PeV)	$E^{95\%}_{\rm cut}$ (PeV)	$E^{(1)}_{\rm LIV}$ (eV) $\times10^{32}$	$E^{(2)}_{\rm LIV}$ (eV) $\times10^{23}$	$E^{(2)}_{\rm LIV}$ (3γ) (eV) $\times10^{25}$
Crab Nebula	2.0	0.88 ± 0.11	$0.75^{+0.04}_{-0.04}$	$4.04^{+0.69}_{-0.62}$	$5.5^{+0.61}_{-0.58}$	$1.04^{+0.11}_{-0.10}$
J2032+4102	1.4	1.42 ± 0.13	$1.14^{+0.06}_{-0.06}$	$14.2^{+2.42}_{-2.18}$	$12.7^{+1.41}_{-1.34}$	$2.21^{+0.23}_{-0.22}$

$E_{planck} = 1.22*10^{19}$ GeV

$10^5\ E_{planck}$ $0.1\%\ E_{planck}$

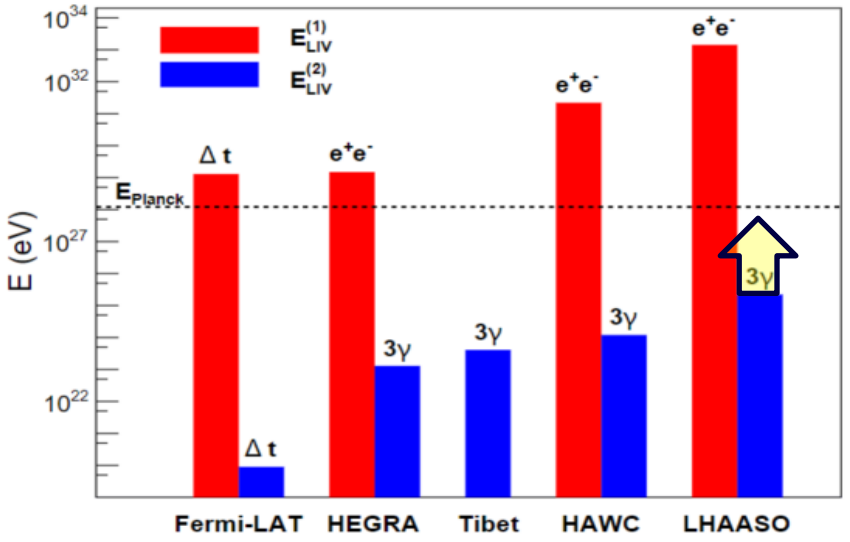

3 orders of magnitudes below the Planck-scale

LHAASO Coll., PRL 128, 051102 (2022)

新物理探索：寻找暗物质

LHAASO观测结果对超重暗物质给出最强限制

- 利用LHAASO基于银盘以外超高能伽马射线测量，**对超重暗物质的寿命下限**做出了迄今**最强烈的限制**，比**已有结果提高了近10倍**，并排除了超重暗物质对超高能弥散中微子观测结果解释的大部分参数范围
- 2022年12月发表，被**物理评论快报**（PRL）编辑选为**高亮论文**

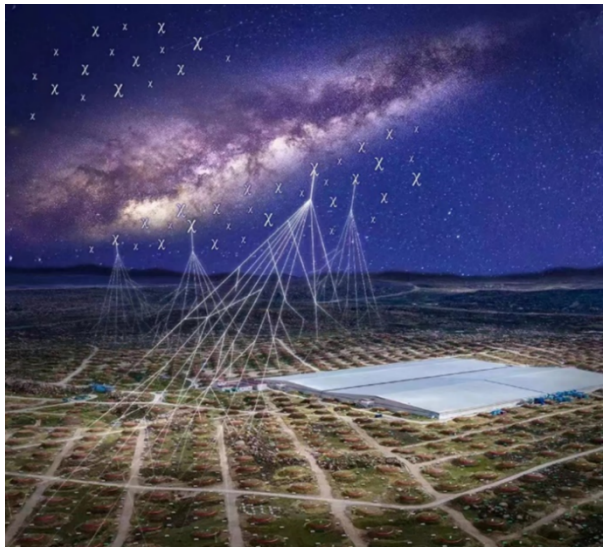

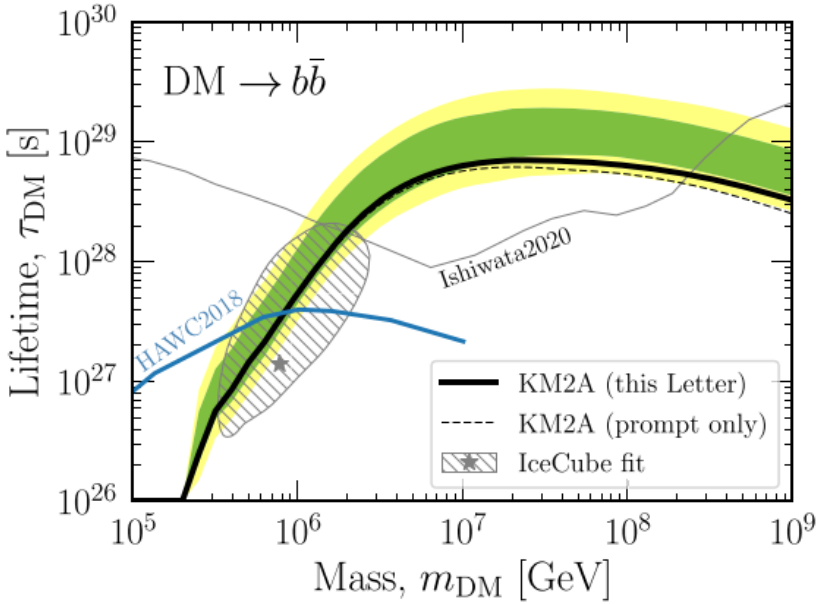

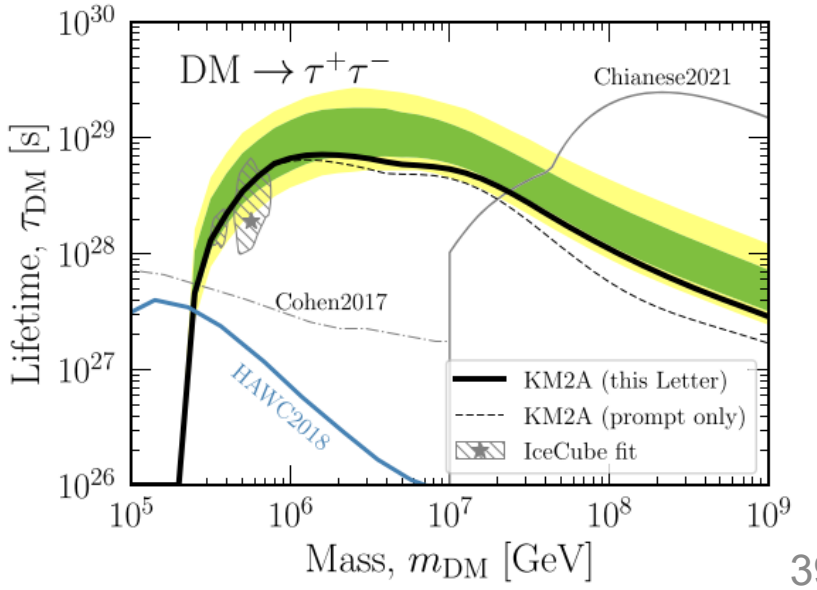

拉索提升计划：大型超高能伽马源立体跟踪装置（LACT）

- LACT：**角分辨比“拉索”提升5倍以上**
  灵敏度和“拉索”相当
- 项目得到四川省委、省政府的大力支持
  已获得了省发改委批复立项
  预算1.5亿
- **媲美欧美部署的耗资2亿欧元的同类项目（CTA）**引起了全球高度关注；
- LACT将**率先**实现对“拉索” 发现的重要天体开展精细结构解析，把握**突破性发现**的重要机遇；
- **“拉索” + LACT 进一步加固了**我国在超高能伽马天文研究领域**的领先地位**；

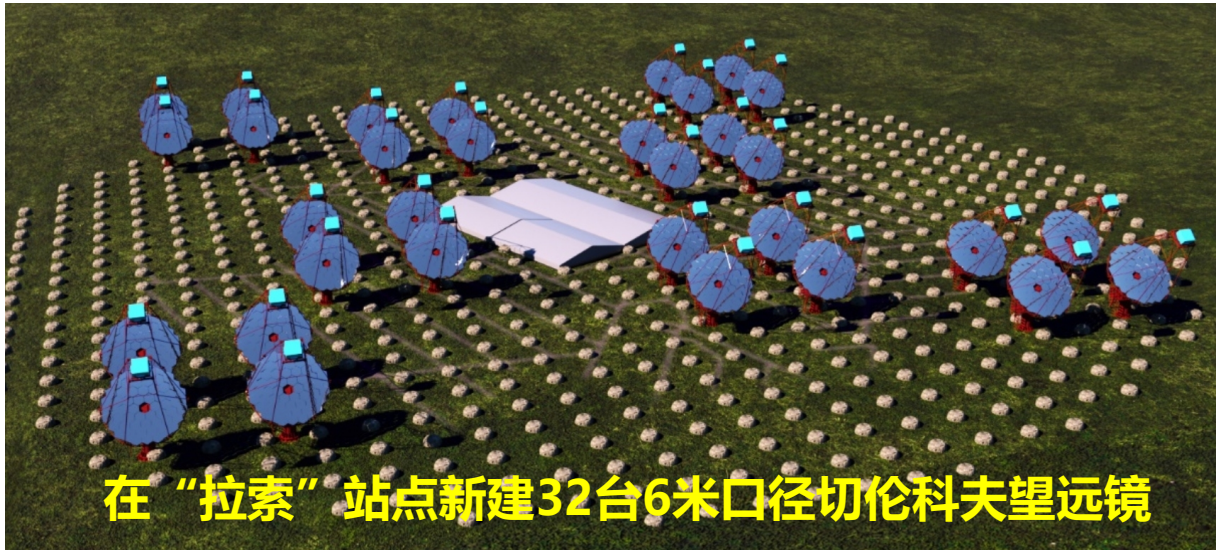

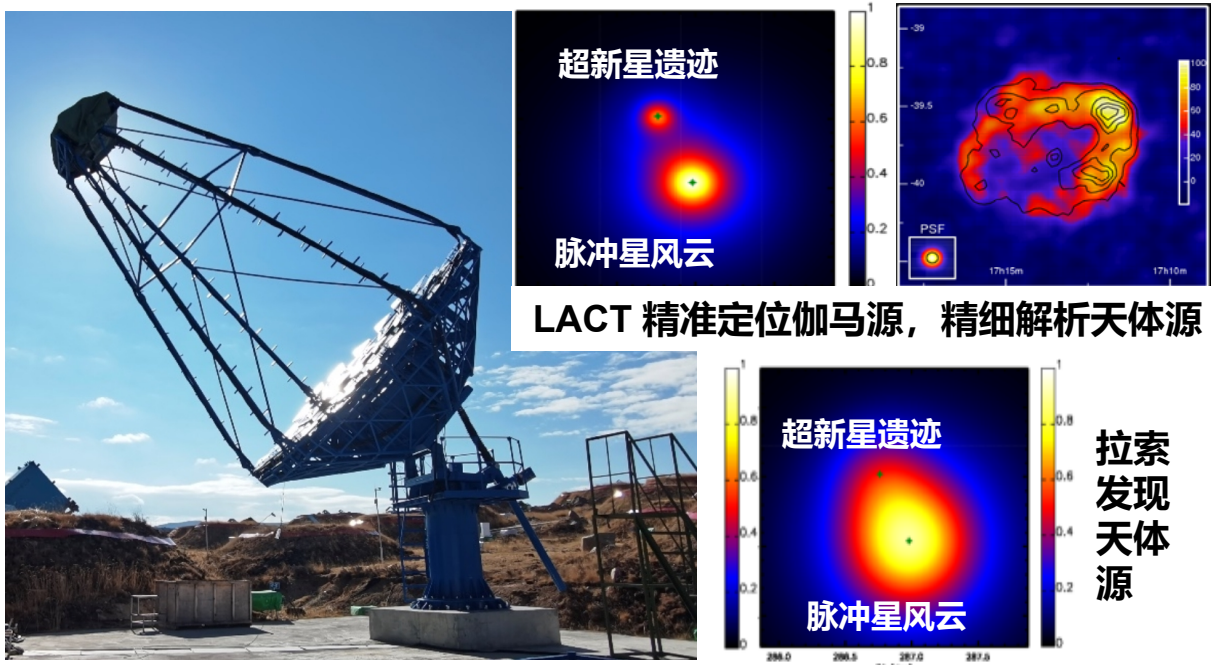


科学探索
未来可期，亦不可期
谢谢！

第一次精确测定“膝”与成分关联

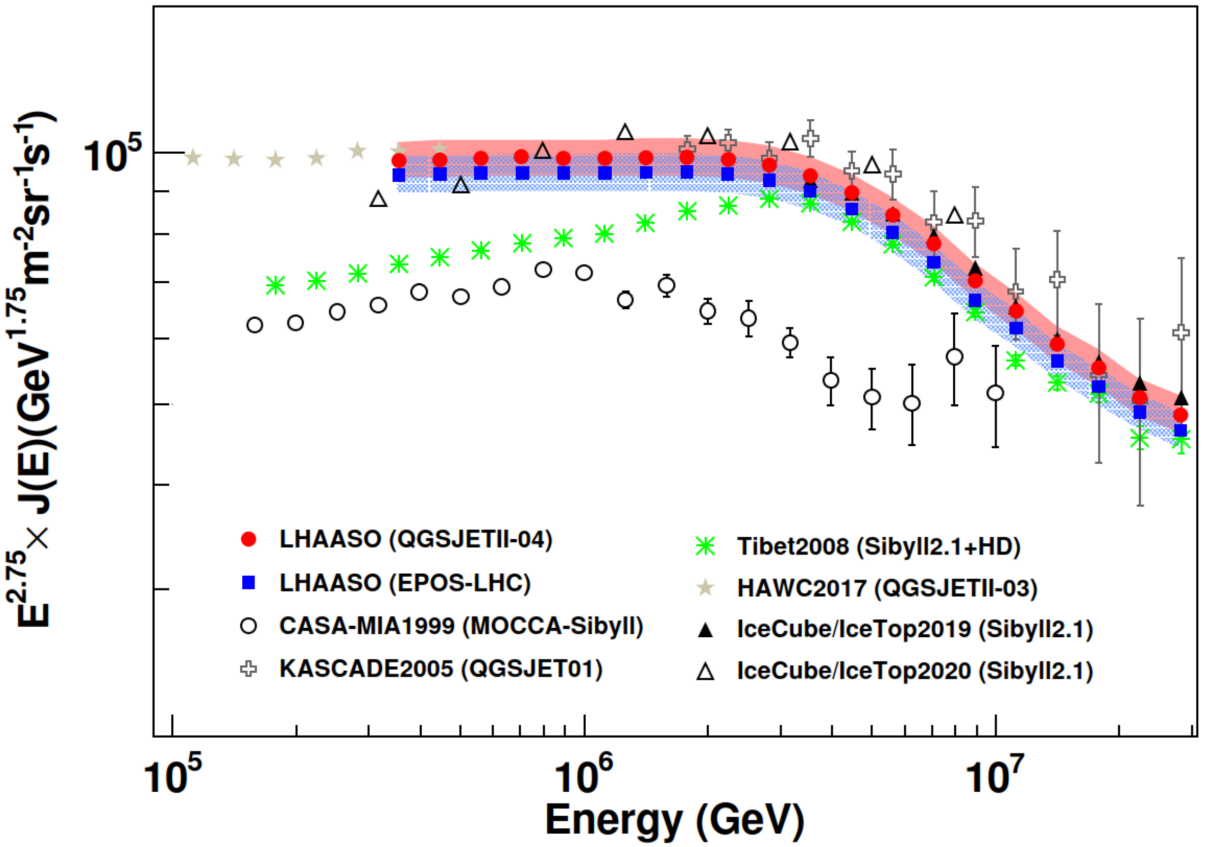

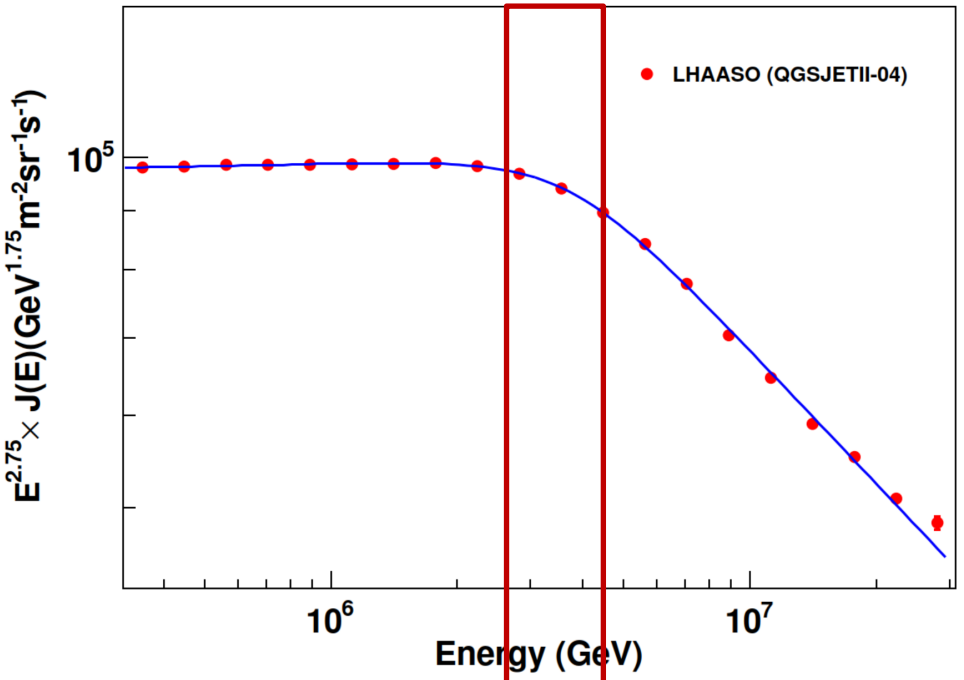

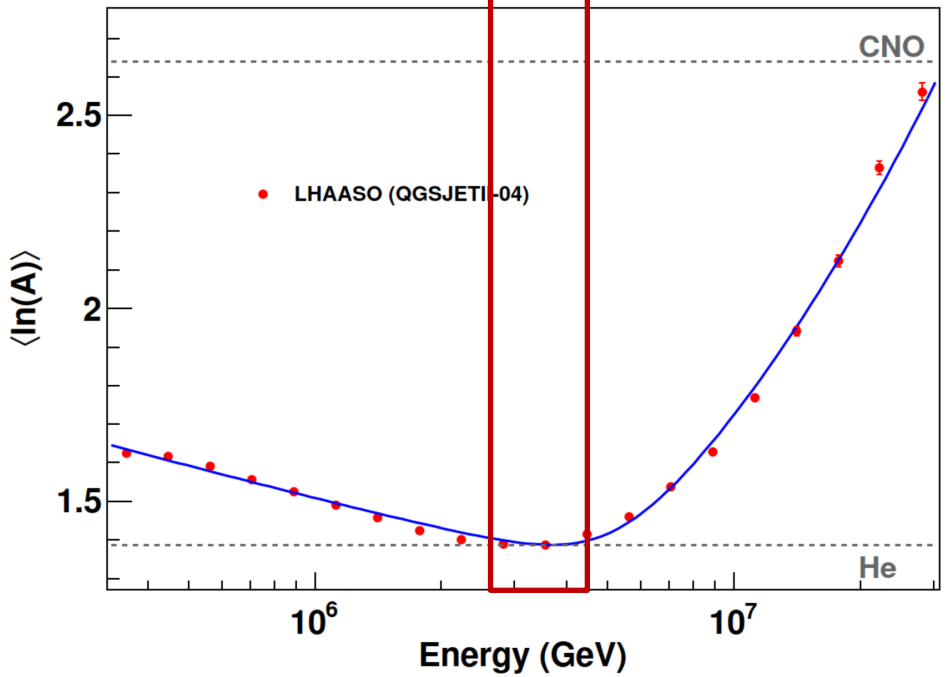

Component sensitive parameters

Muons and electromagnetic particles in EAS

$$N_\mu \propto A^{1-\beta}\left(\frac{E_0}{1\ \mathrm{PeV}}\right)^{\beta}$$

$$N_e \propto A^{1-\alpha}\left(\frac{E_0}{1\ \mathrm{PeV}}\right)^{\alpha}$$

J. R. Hörandel, Cosmic rays from the knee to the second knee: 10^{14} to 10^{18} eV, Mod. Phys. Lett. A 22, 1533 (2007)

$$\log A = \frac{\alpha}{\alpha-\beta}\log\left(\frac{N_\mu}{N_e^{\beta/\alpha}}\right) - \frac{\alpha}{\alpha-\beta}\log\left(\frac{K_\mu}{K_e^{\beta/\alpha}}\right)$$

$$= \frac{\alpha}{\alpha-\beta}\log\left(\frac{N_\mu}{N_e^{\beta/\alpha}}\right) + \mathrm{const}$$

$$\boldsymbol{P_{\mu e} = \log_{10}\frac{N_\mu}{N_e^{0.82}}}$$

- N_μ: 40~200 m
- N_e: 40~200 m

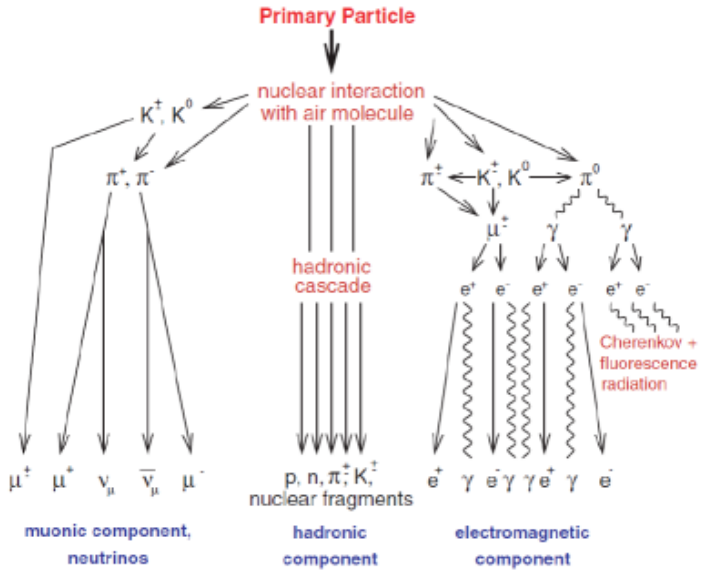

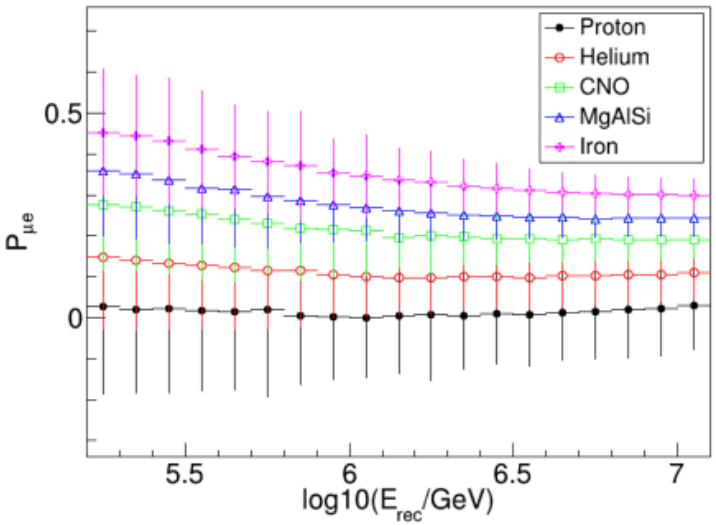

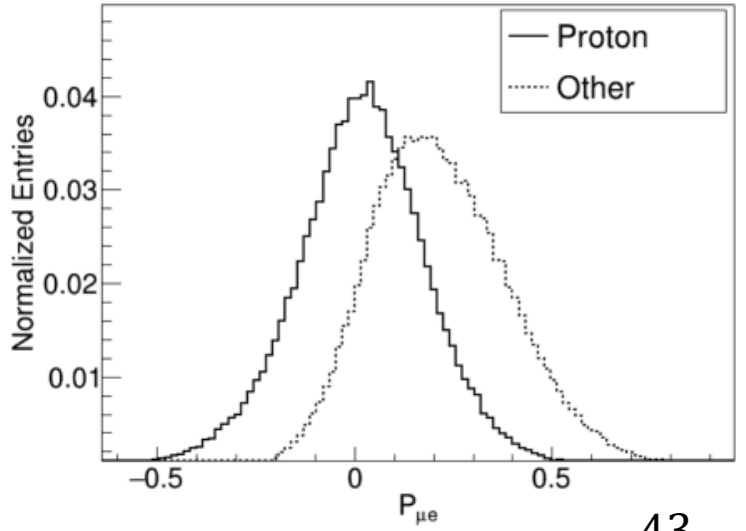

Component sensitive parameters

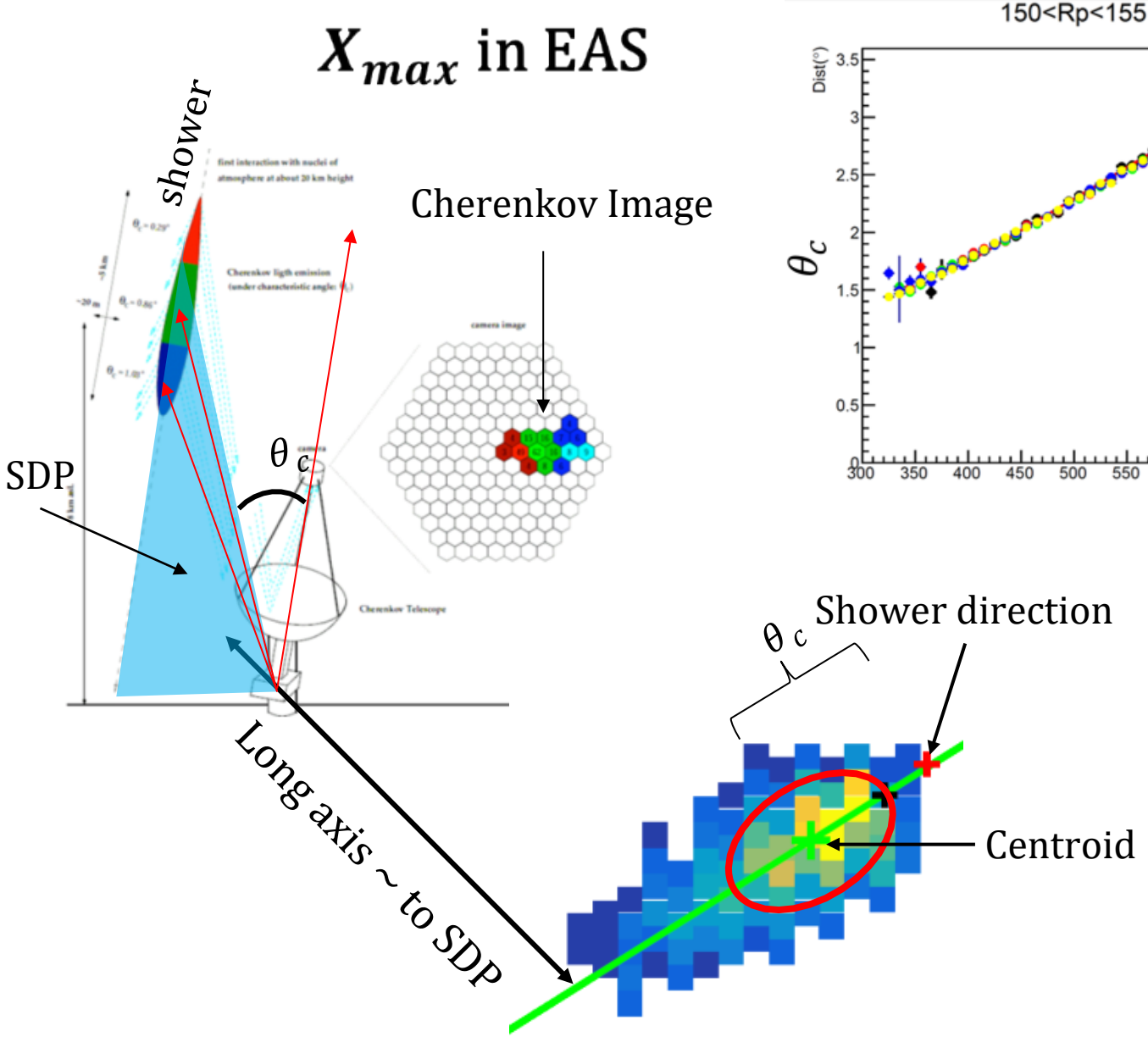

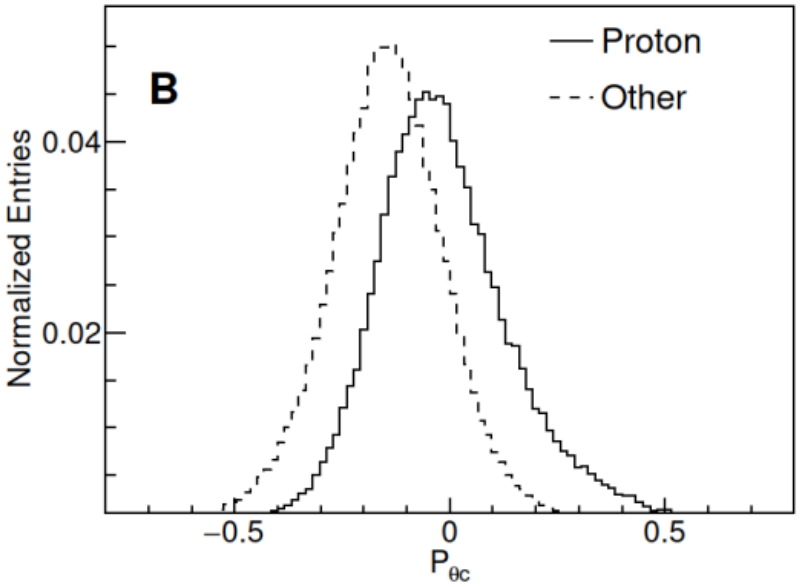

$$P_{\theta c} = \frac{\theta_c^{250} - \langle \theta_c^{250} \rangle}{\langle \theta_c^{250} \rangle|_{PeV}}$$

- Normalization in the impact parameter R_p:

$$\theta_c^{250} = \frac{\theta_c}{\cos(\theta)} + 0.011 \times (R_p - 250)$$

- Normalization in energy:

$$\langle \theta_c^{250} \rangle = p_0 + p_1 \cdot \log_{10} E + p_2 \cdot \log_{10}^2 E$$

- $\langle \theta_c^{250} \rangle|_{PeV}$: the average value of θ_c for proton events at R_p =250 m and E=1 PeV